

How black hole mimickers and Shapiro-free lenses signal effective dark matter

Lirui Yang,^{1,2,3,*} Will Barker,^{4,1,2,†} Tobias Mistele,^{5,‡} and Amel Durakovic^{4,6,7,§}

¹Kavli Institute for Cosmology, Madingley Road, Cambridge CB3 0HA, UK

²Astrophysics Group, Cavendish Laboratory, JJ Thomson Avenue, Cambridge CB3 0HE, UK

³Kavli Institute for Astronomy and Astrophysics, Peking University, Beijing 100871, China

⁴Central European Institute for Cosmology and Fundamental Physics,
Institute of Physics of the Czech Academy of Sciences, Na Slovance 1999/2, 182 00 Prague 8, Czechia

⁵Department of Astronomy, Case Western Reserve University,
10900 Euclid Avenue, Cleveland, Ohio 44106, USA

⁶Observatoire Astronomique de Strasbourg - UMR 7550,
11 rue de l'Université, 67000 Strasbourg, France

⁷Faculty of Science, University of Sarajevo, Zmaja od Bosne 33-35, 71000 Sarajevo, Bosnia-Herzegovina

We report the existence of two exotic compact objects in the leading relativistic model of modified Newtonian dynamics, namely æther-scalar-tensor theory. This model is consistent with precision cosmology and gravitational wave constraints on tensor speed. Black hole mimickers could subtly change observations: gravitational waves from their mergers might show unusual echoes or altered ringdown patterns, and images of their horizon-scale shadows might be slightly different from those of a true black hole. Shapiro-free lenses are massless objects that deflect light without any gravitational time delay, producing distinctive lensing events. These predictions connect to ongoing and future gravitational-wave searches, horizon-scale imaging, and time-domain lensing surveys.

CONTENTS

I INTRODUCTION

I	Introduction	1
II	Theoretical development	4
	<i>A Overview of theories</i>	4
	<i>B Relevant solutions</i>	5
	<i>C Overview of equations</i>	6
III	Asymptotically flat cases	7
	<i>A New branches of exact solutions</i>	8
	<i>B Connection to previous branches</i>	10
IV	Cosmological case	10
V	Conclusions	11
	References	14
A	Details of covariant equations	15
B	Details of component equations	16
C	Conservation of æther acceleration	18
D	Details of exact solutions	19
E	More like black holes than wormholes	22

Dark matter. — The standard dark-energy/cold-dark-matter (ΛCDM) model of cosmology, based in part on general relativity (GR), has been successful on cosmological scales. On smaller galactic scales we observe a tight correlation between the visible, baryonic mass and dark matter, summarised in the baryonic Tully–Fisher relation [1, 2] and the radial acceleration relation [3–5]. Another explanation for these correlations is in terms of new dynamics at low accelerations, i.e., modified Newtonian dynamics (MOND) [6–8]. MOND by itself, however, is concerned only with the non-relativistic limit, i.e. it is an alternative to Newtonian gravity, not an alternative to GR. Thus, various relativistic models that reduce to MOND have been proposed [9], most notably æther-scalar-tensor (ÆST) theory [10]. ÆST stands out as the first model that is consistent with precision observations of the microwave background/large scale structure, and with gravitational waves (GWs) implying a fast tensor mode, while allowing for a MOND-like phenomenology [3, 11]. The phenomenology of ÆST has so far been explored relatively little, however, in the strong-field regime relevant to compact objects. Previous works have considered neutron stars [12, 13], unstable solutions [14], and ‘stealth’ black holes (BHs) which are indistinguishable from BHs in GR [15]. In this work we propose two more exotic compact objects with relatively subtle observational signatures: BH mimickers are hard to *distinguish* from GR BHs, and lenses without Shapiro delay are hard to see *at all*. We are not obliged to put these objects forwards as dark matter candidates, since ÆST is designed already to provide the necessary *effective* dark matter. Rather, their distinct characteristics, if observed, would offer a smoking gun for ÆST itself.

* ly344@cantab.ac.uk

† barker@fzu.cz

‡ txm523@case.edu

§ amel.durakovic@pmf.unsa.ba

Confidence in black holes. — We know that objects of BH density are very common. Doppler shifts in many X-ray binaries indicate $\gtrsim 3 M_\odot$ companions too heavy for neutron stars [16, 17]; astrometry near the compact radio source Sgr A* indicates $\sim 10^6 M_\odot$ contained within $\sim 10^2$ AU of the galactic centre [18, 19] (indeed, modern galaxy evolution is founded on accretion near such supermassive compact objects [20, 21]). Three lines of evidence suggest, moreover, that these BH candidates have horizons as predicted by GR. Firstly, they lack a visibly accreting surface, which would glow thermally or otherwise be illuminated by Type I X-ray bursts [22, 23]. Secondly, GWs from mergers seen by LIGO/Virgo indicate ringing down of quasi-normal modes consistent with a Kerr-type horizon; the GWs appear moreover to be free from surface echos, and can be parameterised by mass and spin [24, 25]. Thirdly, direct VLBI imaging of Sgr A* and M87* by the EHT reveals shadows similarly consistent with Kerr spacetime [26–28]. These methods also constrain the strong-field geometry to nearly Kerr above the horizon, through the circularity of the directly imaged photon ring, inspiral phasing of merger GWs, and Fe K α X-ray emission near the innermost stable circular orbit (ISCO) [24, 28–30]. Astrometric measurements of precession and gravitational redshift near Sgr A* are less stringent, but consistent with at least the Schwarzschild exterior [31, 32]. In summary, exotic objects which only *mimick* BHs face a comprehensive battery of tests. Nonetheless, $\mathcal{A}EST$ contains a strong mimicker candidate (see Fig. 1). These may exist alongside the genuine ‘stealth’ BHs of $\mathcal{A}EST$, which themselves are less diagnostically useful.

Black hole mimickers. — We propose the BH mimicker of $\mathcal{A}EST$ to be a highly asymmetric wormhole, leading only to a BH-type object on its ‘interior’ side. To keep our key results within in this opening section, we quote here our predicted line element on the ‘exterior’ side, i.e. that which is most relevant to observations. For reference, in GR with Newton–Cavendish constant G , the Schwarzschild BH of mass M is described by

$$ds^2 = -\left(1 - \frac{2GM}{r}\right) dt^2 + \frac{dr^2}{\left(1 - \frac{2GM}{r}\right)} + r^2 d\Omega^2, \quad (1)$$

where $d\Omega^2 \equiv d\theta^2 + \sin^2(\theta)d\phi^2$ is the angular measure. The ‘exterior’ side of our mimicker generalises Eq. (1) to

$$ds^2 = -e^{2\mathcal{N}(r)} dt^2 + e^{2\mathcal{M}(r)} dr^2 + r^2 d\Omega^2. \quad (2)$$

Whilst Eq. (1) would imply $\mathcal{N}(r) = -\mathcal{M}(r)$, the BH mimicker instead requires the cumbersome relation

$$e^{2\mathcal{N}(r)} = \left[\frac{\sqrt{2} - \sqrt{2 - K_B^{\text{eff}}}}{\sqrt{2} + \sqrt{2 - K_B^{\text{eff}}}} \right] \times \frac{\sqrt{2 + K_B^{\text{eff}}(e^{2\mathcal{M}(r)} - 1)} + \sqrt{2 - K_B^{\text{eff}}}}{\sqrt{2 + K_B^{\text{eff}}(e^{2\mathcal{M}(r)} - 1)} - \sqrt{2 - K_B^{\text{eff}}}} \sqrt{\frac{2}{2 - K_B^{\text{eff}}}} \quad (3)$$

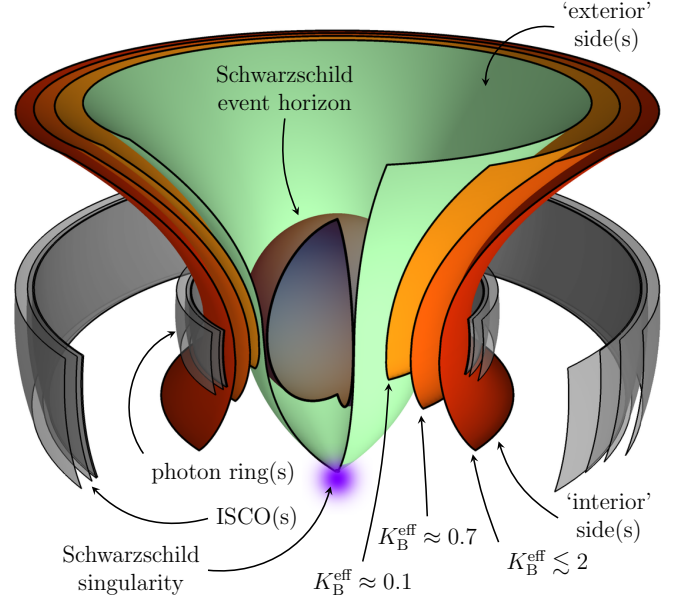


FIG. 1. Embedding visualisation of spatial geometry. Black hole mimickers in $\mathcal{A}EST$ (orange/red, see Eqs. (2) to (4)) emulate the Schwarzschild geometry (green, see Eq. (1)) with the same Newtonian mass M , but have slightly dilated features and a narrow wormhole throat instead of an event horizon. An alternative horizon lies on the ‘interior’ side (here truncated).

The formula in Eq. (3) depends strongly on the dimensionless parameter $K_B^{\text{eff}} < 2$. For the moment, it suffices to know that K_B^{eff} depends on (i) two of the constant $\mathcal{A}EST$ model parameters and (ii) some dynamically acquired flux of scalar hair. The actual formula for $\mathcal{M}(r)$ is defined as being the *inverse* of an ‘ $r(\mathcal{M})$ ’ formula

$$r = \frac{G_N M K_B^{\text{eff}} e^{\mathcal{M}(r)}}{\sqrt{4 + 2K_B^{\text{eff}}(e^{2\mathcal{M}(r)} - 1)} - 2} \left[\frac{\sqrt{2} + \sqrt{2 - K_B^{\text{eff}}}}{\sqrt{2} - \sqrt{2 - K_B^{\text{eff}}}} \right] \times \frac{\sqrt{2 + K_B^{\text{eff}}(e^{2\mathcal{M}(r)} - 1)} - \sqrt{2 - K_B^{\text{eff}}}}{\sqrt{2 + K_B^{\text{eff}}(e^{2\mathcal{M}(r)} - 1)} + \sqrt{2 - K_B^{\text{eff}}}} \sqrt{\frac{1}{4 - 2K_B^{\text{eff}}}}, \quad (4)$$

where the Newtonian G_N in Eq. (4) is also shifted relative to the bare G in Eq. (1) by $\mathcal{A}EST$ model parameters. The take-home point is that Eqs. (2) to (4) ‘mimick’ Eq. (1) to arbitrary precision as $K_B^{\text{eff}} \rightarrow 0$. This is illustrated in Fig. 1, which shows a faithful embedding of 2D equatorial constant-time slices in 3D space.¹ Where the Schwarzschild geometry has an event horizon, however, the BH mimicker always has a slight throat, on the

¹ This is a common method of visualisation: the 3D cylindrical line element $dz^2 + d\rho^2 + \rho^2 d\phi^2$ is equated with Eqs. (1) and (2) at $t = \text{const.}$ and $\theta = \pi/2$. By identifying r with ρ , one gets an equation for $dz/d\rho$ describing the 2D embedded surface.

‘interior’ side of which lies a null singularity. We imagine BH mimickers as accounting for some clandestine fraction of the observed BH population. They would presumably evade all radio, astrometric and GW bounds on the external geometry, and all optical, X-ray and GW bounds on surface characteristics. Signals for BH mimickers from $\mathcal{A}EST$ may include (i) corrections to radio imaging within the photon ring from ‘interior’-side emissions, and (ii) non-BH ringdown.

Confidence in lenses. — We will also be interested in hard-to-find exotic objects that do *not* mimic BHs, but whose subtle lensing properties would provide a smoking gun for $\mathcal{A}EST$ (see Fig. 2) [33, 34]. Statistical microlensing campaigns (MACHO, EROS, OGLE) constrain the fraction of compact lenses in galactic halos across $10^{-7} M_\odot$ to $10 M_\odot$ to below a few percent of CDM [35, 36], while forthcoming wide-field surveys (LSST) will extend sensitivity to sub-lunar masses [37, 38]. Pulsar timing constrains populations of exotic lenses which have become entrained in binary systems. Precision monitoring of binary pulsars — most notably the Hulse–Taylor and subsequent millisecond systems — has confirmed the Shapiro delay (lensing in time) predicted by GR to sub-percent accuracy [39, 40]. No anomalous timing residuals attributable to scalar charges or exotic multipole structure have been observed in existing systems [41, 42]. Pulsar timing arrays (NANOGrav, EPTA, PPTA) likewise report a stochastic background consistent with a population of supermassive BH binaries and show no non-quadrupolar radiation or unexpected spectral features [43, 44]. Notice, however, how all these constraints presume CDM-type lenses, which ‘weigh’ and thus participate in Newtonian gravity. Recalling, therefore, that we have no need of dark matter candidates in $\mathcal{A}EST$, this motivates considering an extreme case: a ‘weightless’ gravitational lens.

Shapiro-free lenses. — We propose a ‘weightless’ lens in $\mathcal{A}EST$ which — though it is *not* a wormhole — is inspired by the line element of the massless Ellis–Bronnikov wormhole [45, 46]. The Ellis–Bronnikov wormhole is given by the ‘(+)’ configuration in

$$ds^2 = -dt^2 + dr^2 + (r^2 \mp \ell^2) d\Omega^2, \quad (5)$$

where t and r are now the proper time and radius. As popularised by Visser [47, 48], Morris and Thorne [49, 50], the ‘(+)’ configuration is a far less subtle wormhole than the BH mimicker, with correspondingly more applications in science fiction: it seemingly allows test geodesics to pass between two asymptotically flat regions via a ‘throat’ of minimal area $4\pi\ell^2$ at $r = 0$, which needs to be held open by phantom matter in the Einstein field equations. By contrast, our ‘Shapiro-free lens’ is the ‘(−)’ configuration of Eq. (5), which requires no phantom matter, being an exact solution to the $\mathcal{A}EST$ field equations in which the wormhole throat closes up. This promotes the object from a formal curiosity to a subtle observational challenge. Its constant-time hypersurfaces

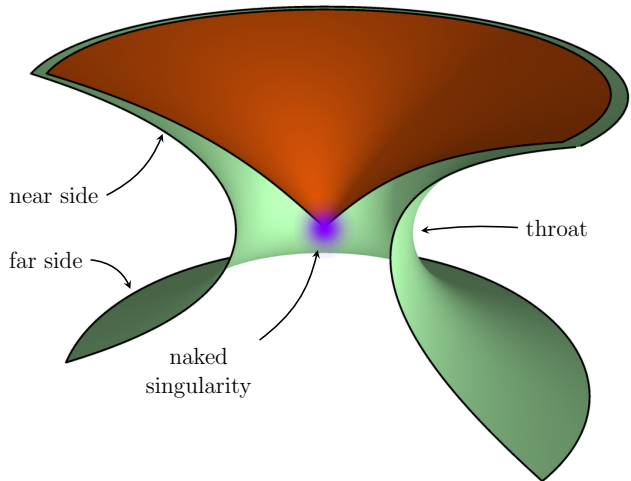


FIG. 2. Embedding visualisation of spatial geometry. Lenses without Shapiro delay in æther-scalar-tensor theory (red, see ‘(−)’ configuration in Eq. (5)) are massless regions of curved space ending in a naked singularity. They are the analytic continuation of Ellis wormholes (green, see ‘(+)’ configuration in Eq. (5)).

are highly curved, as illustrated in Fig. 2 — indeed this figure captures the *full* Riemannian curvature, which has no ‘time part’ whatever (so-called *ultrastaticity*²). The object thus has no mass M at infinity, no gravitational redshift, and indeed *no gravity*. A naked singularity (or star-like matter configuration) sources the scalar hair and sets ℓ , but it does not accrete, and whilst its spatial curvature gives rise to lensing, the lensed rays experience no Shapiro delay. This is a result of the object being more compact than its Schwarzschild equivalent: its Weyl potential, relevant for lensing, scales as $\sim 1/r^2$, rather than $\sim 1/r$ as in GR. The Shapiro delay incurred by integrating the tails of this potential is thus not enhanced (as the case in GR) by a logarithmic divergence in the source-observer distance: it is this logarithm that usually dominates in cosmological lenses. Besides lacking the logarithmic contribution, Shapiro delay is suppressed in a more general sense, as follows. The delay in GR is proportional overall to $2GM$, which is seen in Eq. (1) to be the gravitational scale of the lens. The new kind of lens in the ‘(−)’ configuration of Eq. (5) has a gravitational scale of ℓ , but its Shapiro delay is proportional to ℓ^2/b , where b is the impact factor. Thus, for the new lens to induce comparable Shapiro delay at the same b to a GR lens, its scale must be $\ell \sim \sqrt{2GMb}$. For all astronomical lenses $b \gg 2GM$, implying a large geometric mean $\ell \gg 2GM$. To give a concrete exam-

² Ultrastatic spacetime is not only static, in the sense that it has a global timelike Killing vector, but additionally this Killing vector has unit norm [51]. The general ultrastatic line element takes the form $ds^2 = -dt^2 + g_{ij} dx^i dx^j$. On the slices defined by $t = \text{const.}$ additionally have no extrinsic curvature.

ple, one would need $\ell \sim 10^3$ km to comparably perturb sun-grazing radar pulses (as in Shapiro’s original experiment [52, 53]), i.e., three orders of magnitude larger than a solar-mass black hole. This separation of scales is ten times more severe in the microlensing context, where we imagine actually searching for such objects. In this case, another concrete example is given by primordial BHs of $M \sim 10 M_\odot$, which are a popular focus in microlensing: their magnification of sources in the Milky Way region would be apparent within an Einstein radius of $b \sim 10$ AU. Such a microlensing event would need to be explained by a ‘large’ object of $\ell \sim 10^5$ km, i.e., four orders of magnitude larger than the BH. Thus, assuming that Λ EST gives rise to a population of more ‘reasonably sized’ lenses, the microlensing implications are expected to be very subtle.³ Besides being weaker, the Weyl potential also has the ‘wrong’ sign, akin to negative mass in GR. The Shapiro delays that do arise would thus be *negative*, in that signals would be slightly advanced, not retarded. We can understand why this happens heuristically, from the ‘(−)’ configuration in Eq. (5). The lensed rays are traversing a spherical excision of radius ℓ , that has then been ‘sewed-up’. In some sense, they are taking a short-cut through a piece of space that has been removed. The angular deflection also carries the ‘wrong’ sign, so that the object is optically repulsive. To summarise, a population of such lenses (e.g. early-Universe relics) would thus seem hard — but not impossible — to observe, and their unusual characteristics would provide a clear signal for Λ EST.

In this work. — Our objective is to show that (i) the exact solutions proposed in Eqs. (2) to (5) do indeed satisfy the Λ EST field equations, and (ii) that they have the above phenomenological properties. In particular whilst the mimicker solution does evidently have a Newtonian limit, we will not be overly concerned with matching either the mimicker or the lens to the MOND regime, because the question of strong- and weak-field matching in Λ EST is not yet well understood: there is a generic expectation that this matching process is intimately connected with the dynamical history of the system. Two aspects need to be investigated in further work. Firstly, dynamical production and stability against perturbations, in the context of cosmological/astrophysical backgrounds and timescales, leading to abundance predictions. Secondly, computation of precise observational signatures leading to multi-messenger forecasts. In Section II C we will obtain the field equations of Λ EST. In Section III we obtain the compact solutions, with a cosmological solution in Section IV. We conclude in Section V. Technical appendices follow, including two of general interest. In Appendix C, we show that the acceleration of static æther

is *generally* a conserved current. In Appendix E we show that the BH mimicker is a wormhole *in name only*: instead of leading to another universe, it leads to a singular Killing horizon.

Conventions. — We try to match [10, 54], using the signature $(-, +, +, +)$, and natural units $c \equiv \hbar \equiv 1$. Further conventions are introduced as needed.

II THEORETICAL DEVELOPMENT

A. Overview of theories

Scalar-tensor theory. — The simplest extension of GR is the massless scalar-tensor theory

$$S_{\text{ST}} \equiv \int d^4x \frac{\sqrt{-g}}{2\kappa} \left[R \mp \nabla_\mu \varphi \nabla^\mu \varphi \right], \quad (6)$$

where R is the Ricci scalar,⁴ and $\kappa \equiv 8\pi G$ is the Einstein constant with G the Newton–Cavendish constant. The shift-symmetric scalar φ is made dimensionless in Eq. (6), and with our signature the ‘(±)’ sign allows canonical ‘(−)’ or phantom ‘(+)’ character. One of our key findings will be that this primitive class of models goes a long way towards explaining the solutions of Λ EST, even though the latter is a far more intricate model. This is especially surprising, because whilst Λ EST also contains a shift-symmetric scalar φ , the operators of this field are everywhere entangled with an additional dimensionless vector field A^μ , which has an æther character.

Einstein-æther theory. — By contrast with the scalar-tensor theory of Eq. (6), the simplest æther model is Maxwell-type Einstein-æther (EÆ) theory [55, 56]. The action, using $F_{\mu\nu} \equiv \nabla_\mu A_\nu - \nabla_\nu A_\mu$, is given by

$$S_{\text{EÆ}} \equiv \int d^4x \frac{\sqrt{-g}}{2\kappa} \left[R - \frac{K_{\text{B}}}{2} F^{\mu\nu} F_{\mu\nu} - \lambda (A^\mu A_\mu + 1) \right], \quad (7)$$

where the dimensionless æther coupling lies in the range

$$0 < K_{\text{B}} < 2, \quad (8)$$

mandated by the stability of perturbations.⁵ The general idea is to identify a preferred frame at each point in the spacetime as having a four-velocity given by the

³ Ultimately, until the formation of Shapiro-free lenses is understood, the question of whether or not a given value of ℓ is ‘reasonable’ is still speculative, and the scales of primordial BHs simply offer a familiar benchmark.

⁴ Our conventions are $R \equiv R^\mu_\mu$ for the Ricci tensor $R_{\mu\nu} \equiv R^\sigma_{\mu\sigma\nu}$, where the Riemann tensor is $R^\sigma_{\rho\mu\nu} \equiv \partial_\mu \Gamma^\sigma_{\rho\nu} - \partial_\nu \Gamma^\sigma_{\rho\mu} + \dots$ and $\Gamma^\mu_{\nu\rho} \equiv g^{\mu\sigma} (\partial_\nu g_{\rho\sigma} - \frac{1}{2} \partial_\sigma g_{\nu\rho})$ is the Christoffel symbol.

⁵ Note in particular that the solutions to the EÆ field equations are not always continuous as $K_{\text{B}} \rightarrow 0$, though as a rule of thumb the EÆ phenomenology coincides with pure GR in this limit.

vector field A^μ . For this interpretation to hold, the vector must be everywhere timelike and with unit length: these conditions are ensured in Eq. (7) by the dynamics of λ , which is a Lagrange multiplier. Ignoring the multiplier terms leads back to Einstein–Maxwell theory in which $\sqrt{K_B/\kappa}A^\mu$ is the electromagnetic gauge potential.

Æther-scalar-tensor theory. — Going beyond scalar-tensor and EÆ theories, ÆST blends the dynamics of φ and A^μ through the action

$$S_{\text{ÆST}} \equiv \int d^4x \frac{\sqrt{-g}}{2\kappa} \left[R - \frac{K_B}{2} F^{\mu\nu} F_{\mu\nu} + 2(2 - K_B) J^\mu \nabla_\mu \varphi - (2 - K_B) \mathcal{Y} - \mathcal{F}(\mathcal{Y}, \mathcal{Q}) - \lambda (A^\mu A_\mu + 1) \right], \quad (9)$$

where, as in EÆ theory, we assume Eq. (8) for reasons of stability [57]; the other quantities in Eq. (9) are defined

$$J_\mu \equiv A^\nu \nabla_\nu A_\mu, \quad q_{\mu\nu} \equiv g_{\mu\nu} + A_\mu A_\nu, \quad (10)$$

$$\mathcal{Q} \equiv A^\mu \nabla_\mu \varphi, \quad \mathcal{Y} \equiv q^{\mu\nu} \nabla_\mu \varphi \nabla_\nu \varphi.$$

In particular, if A^μ is interpreted as the four-velocity of the preferred frame, then it follows from Eq. (10) that J^μ must be the four-acceleration of that frame. In general, $\mathcal{F}(\mathcal{Y}, \mathcal{Q})$ is a free function of the scalars \mathcal{Y} and \mathcal{Q} . One motivated form for this function was proposed in [10], whereby

$$\mathcal{F}(\mathcal{Y}, \mathcal{Q}) = (2 - K_B) \mathcal{J}(\mathcal{Y}) - \mathcal{F}_{20} (\mathcal{Q} - \mathcal{Q}_0)^2, \quad (11)$$

where \mathcal{Q}_0 has mass-dimension one and

$$\mathcal{F}_{20} > 0, \quad (12)$$

is dimensionless. The idea behind Eq. (11) is that the \mathcal{Q} -dependent term is responsible for reproducing a cosmological CDM-like component, while the \mathcal{Y} -dependent term is responsible for explaining the missing mass problem in galaxies [10]. Heuristically, \mathcal{Q} carries the time derivatives of the scalar field, while \mathcal{Y} carries the spatial derivatives, so that \mathcal{Q} is relevant in time-dependent situations (e.g. cosmology) while \mathcal{Y} is relevant to static or quasi-static situations (e.g. galaxies). To reproduce the successes of MOND in describing gravity on galactic scales, the function $\mathcal{J}(\mathcal{Y})$ in Eq. (11) is (somewhat hazily) defined as

$$\mathcal{J}(\mathcal{Y}) \equiv \begin{cases} \lambda_s \mathcal{Y}, & \mathcal{J}(\mathcal{Y}) \gg a_0^2, \\ \frac{2\lambda_s \mathcal{Y}^{3/2}}{3(1+\lambda_s)a_0}, & \mathcal{J}(\mathcal{Y}) \ll a_0^2, \end{cases} \quad (13)$$

where $a_0 \sim 1 \times 10^{-10} \text{ m s}^{-2}$ is the MOND acceleration scale, and the dimensionless parameter λ_s obeys

$$0 < \lambda_s, \quad (14)$$

again to avoid an instability.⁶ In galaxies, Eq. (13) will reproduce Newtonian gravity at accelerations large compared to a_0 , and MOND-like gravity at accelerations small compared to a_0 . In the following we will mostly restrict ourselves to the Newtonian ansatz for $\mathcal{J}(\mathcal{Y})$, which is relevant to small radii, appropriate for BH and wormhole solutions. Without introducing new parameters to modify the Newtonian ansatz, we will find that the strong-field departures from Newtonian phenomena have remarkably promising observational implications. Having already restricted to the minimal quadratic \mathcal{Q} ansatz required for effective CDM, our decision to neglect the MOND ansatz allows us to avoid the further set of arbitrarily many parameters that would interpolate between the two ansätze for $\mathcal{J}(\mathcal{Y})$.⁷ Even with this maximally predictive approach, the prior constraints on the five remaining parameters in ÆST, namely G , K_B , λ_s , \mathcal{F}_{20} and \mathcal{Q}_0 , remain very weak. They include

$$\frac{2(1+\lambda_s)}{\lambda_s(2-K_B)} \mathcal{F}_{20} \mathcal{Q}_0^2 \sim 1 \text{ Mpc}^{-2}, \quad (15)$$

which was arrived at in [11] as a ‘goldilocks’ estimate for producing MOND in galaxies, and suppressing it on the scale of galaxy clusters (see also [58]).⁸ An extra subtlety also affects G (i.e. κ) in Eq. (9), which in ÆST should be considered a *bare* coupling.⁹ The *measured* Newtonian $G_N \approx 6.67 \times 10^{-11} \text{ m}^3 \text{ kg}^{-1} \text{ s}^{-2}$ was derived in [10], and found to be given by the formula

$$G_N \equiv \frac{(1+\lambda_s) 2G}{\lambda_s(2-K_B)}, \quad (16)$$

where G , K_B and λ_s are otherwise unconstrained.

B. Relevant solutions

Ellis–Bronnikov drainhole. — Solutions in scalar-tensor theory have been extensively studied [59–61]. The

⁶ Note that [57] suggests the more conservative bound $1 < \lambda_s$, though the bound given in Eq. (14) is the one most commonly assumed.

⁷ Note that, as initially formulated in terms of arbitrary functions, ÆST is not a predictive model with finitely many parameters; the same problem is seen in $f(R)$ theories.

⁸ In more detail, a value in Eq. (15) $\lesssim 1 \text{ Mpc}^{-2}$ is preferred to avoid oscillatory accelerations in galaxies, which would be predicted by ÆST but which are not observed. Meanwhile, galaxy clusters appear to exhibit an offset from the MOND acceleration relation: this may be explained by $\gtrsim 1 \text{ Mpc}^{-2}$. Only a value $\sim 1 \text{ Mpc}^{-2}$ is consistent with both regimes.

⁹ The theories Eqs. (6), (7) and (9) are all assumed to be low-energy effective theories. Our use of ‘bare’ has nothing whatever to do with renormalisation, and means only that the classical dynamics of the æther and scalar impose further modifications to the Newtonian limit, beyond GR.

phantom ‘(+)’ case of Eq. (6) admits the celebrated two-parameter ‘drainhole’ solution of Ellis [45] and Bronnikov [46] (see also [60–63]). Both sides of this asymmetric wormhole are asymptotically flat. The near side behaves like the Schwarzschild solution at spatial infinity, one of the parameters setting the attractive asymptotic mass; the far side is correspondingly repulsive. The throat of the wormhole is independently dilated by the second parameter. The massless limit is a symmetric, one-parameter wormhole. The absence of a mass means that, throughout the whole spacetime, static observers experience no acceleration. The resulting wormhole has no gravity, and geodesics ‘coast’ freely from one side to the other only if they happen to intersect the throat.

Fisher–JNW solution. — Conversely, if the scalar is canonical, i.e. the ‘(–)’ case of Eq. (6), there is a two-parameter analogue of the Ellis–Bronnikov solution attributed first to Fisher [64] and rediscovered much later by Janis, Newman and Winicour (JNW) [65]. The analogy is exact, in the sense that analytic continuation of the Fisher–JNW solution to the phantom ‘(+)’ case just yields the Ellis–Bronnikov drainhole in different coordinates. Non-phantom Fisher–JNW spacetime is also asymptotically flat, but it contains a naked singularity at its center, not a throat. As with the Ellis–Bronnikov solution, however, there exists a massless limit: the naked singularity persists, but it is weightless, so that static observers are not drawn towards it.

Eling–Jacobson wormhole. — Static, spherical solutions to EÆ theory in Eq. (7) were studied extensively by Eling and Jacobson in [66]. The Eling–Jacobson solution is also massive, with an asymptotically flat near side (which we will think of as an ‘exterior’) consistent with the Newtonian limit of the Schwarzschild solution. The Eling–Jacobson solution, however, does not quite describe a BH, but rather a highly asymmetric wormhole. On the far side (‘interior’) of its throat lies a very different region which is not asymptotically flat, but which ends at a singular Killing horizon. In the $K_B \rightarrow 0$ limit, the throat radius approaches (from above) the value of the Schwarzschild radius associated with the mass, and in fact the whole ‘exterior’-side geometry approaches the Schwarzschild vacuum. Similar spacetime geometries have been found in exact solutions to bumblebee gravity [67], and more recently in exact solutions to ÆST itself [15].

Stealth BH. — Ignoring the multiplier term in Eq. (7) yields Einstein–Maxwell theory. It is sometimes forgotten that a unit-timelike condition on the electromagnetic gauge potential is actually a perfectly valid gauge choice in electromagnetism. Indeed, this *Dirac gauge* was among the earliest motivations for æther models such as the EÆ theory. It is unsurprising, therefore, that one branch of solutions to EÆ theory is actually Reissner–Nordström. Less obvious is the fact that this solution is also inherited by ÆST, as shown recently

in [15]. In the limit of vanishing charge, the Reissner–Nordström geometry cannot be observationally distinguished from that of Schwarzschild, and such field configurations in ÆST have been dubbed ‘*stealth*’ BHs.

C. Overview of equations

Simplified action. — Our starting point for everything that follows will be to refine Eq. (9) by assuming the form proposed by Skordis and Złosnik in Eq. (11). We will not, however, enforce the assumptions in Eq. (13), which lead to MOND phenomenology. We rewrite the action as

$$S_{\text{ÆST}}^{\text{SZ}} \equiv \int d^4x \frac{\sqrt{-g}}{2\kappa} \left[R - \frac{K_B}{2} F^{\mu\nu} F_{\mu\nu} + 2(2 - K_B) J^\mu \nabla_\mu \varphi - \mathcal{V}(\mathcal{Y}) + \mathcal{F}_{20}(\mathcal{Q} - \mathcal{Q}_0)^2 - \lambda(A^\mu A_\mu + 1) \right], \quad (17)$$

so that $\mathcal{J}(\mathcal{Y})$ from Eq. (11) and $(2 - K_B)\mathcal{Y}$ from Eq. (9) are combined into the ‘potential’ $\mathcal{V}(\mathcal{Y})$.

Covariant equations. — The field equations are obtained by taking variations of Eq. (17) with respect to the dynamical degrees of freedom: the metric $g_{\mu\nu}$, the æther field A^μ , the scalar field φ and the Lagrange multiplier λ . Variation with respect to λ yields the normalization constraint on the æther field

$$A^\mu A_\mu = -1. \quad (18)$$

Even after Eq. (18) has been imposed, the remaining field equations (which include among their components propagating equations as well as constraints) remain somewhat cumbersome, and we confine them to Appendix A. Note that the A^μ -equation contains a term of the form $\delta S_{\text{ÆST}}^{\text{SZ}}/\delta A^\mu \supset -\sqrt{-g}\lambda A_\mu/\kappa$, so that after contraction with an extra factor of A^μ followed by an application of Eq. (18) it allows for the Lagrange multiplier λ to be determined algebraically (see Eq. (A4)).

Component equations. — Initially, the line element in the spherically symmetric spacetime is not assumed to be Schwarzschild-like or isotropic; we write

$$ds^2 = -e^{2\mathcal{N}(r)} dt^2 + e^{2\mathcal{M}(r)} dr^2 + \mathcal{R}(r)^2 d\Omega^2, \quad (19)$$

and this provides our ansatz for the metric $g_{\mu\nu}$. The scalar field φ and the æther field A^μ are assumed to share the same spherical symmetry with the spacetime. In the case of the æther field, this means that only temporally and radially aligned components are allowed, and together with Eqs. (18) and (19) this yields

$$[A_\mu] = [\cosh(\alpha(r))e^{\mathcal{N}(r)}, \sinh(\alpha(r))e^{\mathcal{M}(r)}, 0, 0]. \quad (20)$$

Finally, we allow φ to additionally have some time dependence, which is related to the first term in Eq. (11)¹⁰

$$\varphi = \mathcal{Q}_0 \chi(t) + \psi(r), \quad (21)$$

accordingly, we refer to it as $\varphi(t, r)$. The component-level equations following from Eqs. (19) to (21) can be found in Appendix B. From this point on, however, we will focus on the solutions with purely time-aligned æther (the so-called ‘static æther’ condition), by setting

$$\alpha(r) = 0, \quad (22)$$

in Eq. (19).¹¹ Following from Eq. (22) we then find (see discussion in Appendix C)

$$F_{\mu\nu} F^{\mu\nu} = -2J_\mu J^\mu, \quad J_\mu \nabla^\mu \varphi = J_\mu \nabla^\mu \psi, \quad (23)$$

$$\mathcal{Y} = \nabla_\mu \psi \nabla^\mu \psi, \quad \mathcal{Q} = -\mathcal{Q}_0 \frac{d\chi}{dt} e^{-\mathcal{N}}.$$

We will also impose the constraint on Eq. (19)

$$\mathcal{M}(r) = -\mathcal{N}(r). \quad (24)$$

The condition in Eq. (24) can always be met by a suitable rescaling of r . In general, this choice will not coincide with $\mathcal{R}(r) = r$. Accordingly, r need not be tied to the area of enclosing two-spheres, so the resulting coordinates need not be Schwarzschild-like. Note, however, that in general, the r coordinate scaled according to Eqs. (19) and (24) is proportional to the affine parameter of radial null geodesics. When Eqs. (21), (22) and (24) are imposed on the field equations, a constraint from Eq. (B1b) yields (see Appendix D)

$$\mathcal{Q}_0 \left(\left[(2 - K_B) \frac{d\mathcal{N}}{dr} + \left(\mathcal{F}_{20} - \frac{d\mathcal{V}}{d\mathcal{Y}} \right) \frac{d\psi}{dr} \right] \frac{d\chi}{dt} - \mathcal{F}_{20} e^{\mathcal{N}} \frac{d\psi}{dr} \right) = 0, \quad (25)$$

and Eq. (25) will be instrumental in guiding our search for solutions. We will show that the spherically symmetric, static solutions to the ÆST field equations can have both scalar-tensor and EÆ character. In particular, we show that ÆST in Eq. (9) inherits the Eling–Jacobson wormhole of EÆ theory in Eq. (7), but with an ‘effective’ æther coupling K_B^{eff} , which is shifted relative to the bare K_B by the scalar current. This solution forms the basis for our BH mimicker. We will uncover a second branch of solutions for which the æther acceleration J^μ vanishes: this describes an ultrastatic (massless) space-time, and forms the basis for our Shapiro-free lens.

¹⁰ It may seem unlikely that time dependence of φ will lead to exact solutions for which the spacetime geometry is static, but in fact this happens in ÆST for the simplest case of Minkowski spacetime (see detailed discussion in [57]). Heuristically, $\varphi = \mu t + \dots$ introduces a chemical potential μ in a statistical mechanics description of the theory. From this perspective, it is natural to expect static spacetime at equilibrium.

¹¹ The consequences of relaxing this condition are discussed in [68].

III ASYMPTOTICALLY FLAT CASES

Guiding equations. — To obtain asymptotically flat solutions, we need to neglect the MOND regime. Without MOND, by referring to Eq. (13) we see that the function $\mathcal{V}(\mathcal{Y})$ in Eq. (17) is linear, i.e.

$$\mathcal{V}(\mathcal{Y}) = (2 - K_B)(1 + \lambda_s) \mathcal{Y}. \quad (26)$$

Our discussion will be driven in particular by two component-level conditions that arise out of the field equations when the assumptions in Eqs. (21), (22), (24) and (26) are applied. Firstly, it is found that Eq. (B1e) provides a necessary condition for the existence of non-trivial solutions

$$\mathcal{F}_{20} \mathcal{Q}_0 \mathcal{R} \frac{d\psi}{dr} \left(e^{\mathcal{N}} - \frac{d\chi}{dt} \right) = 0. \quad (27)$$

We focus on the case where Eq. (27) is satisfied because

$$\mathcal{F}_{20} \mathcal{Q}_0 = 0. \quad (28)$$

Referring back to Eq. (11), the condition in Eq. (28) implies that we are neglecting the capacity of ÆST to provide a CDM component in the cosmological background and perturbation theory — again, this ought to be safe for strong fields. Secondly, under Eqs. (26) and (28) the complicated constraint in Eq. (25) reduces to

$$\mathcal{Q}_0 \frac{d\chi}{dt} \left(\frac{d\mathcal{N}}{dr} - (1 + \lambda_s) \frac{d\psi}{dr} \right) = 0, \quad (29)$$

which has a much simpler form.

Heuristic action. — When Eqs. (19) to (22), (26) and (28) hold, Eq. (23) can be used to re-write the action in Eq. (17) as¹²

$$S_{\text{ÆST}}^{SZ} \cong \int d^4x \frac{\sqrt{-g}}{2\kappa} \left[R + K_B J^\mu J_\mu - \lambda (A^\mu A_\mu + 1) + (2 - K_B) \left(2J^\mu - (1 + \lambda_s) \nabla^\mu \psi \right) \nabla_\mu \psi \right]. \quad (30)$$

We have verified explicitly that the equations of motion derived from Eq. (30) reproduce the solutions of the original action in Eq. (17), expressed in terms of the metric $g_{\mu\nu}$, the scalar φ , and the vector A^μ , after Eqs. (19) to (22), (26) and (28) are imposed.¹³ We particularly

¹² Note that the existence of a covariant reduced action such as that given in Eq. (30) is not guaranteed in general. For highly symmetric spacetimes, however, one is guaranteed to be able to write a non-covariant minisuperspace action which reproduces valid field equations [69, 70] — we are not using this technique.

¹³ The Lagrange multiplier λ implied by Eq. (30) differs by a constant factor from that implied by the original action. This affects the energy-momentum tensor, to which λ contributes. This change is, however, exactly compensated for by another change, due to the fact that the metric variation of the two (off-shell) expressions $-2J^\mu J_\mu$ and $F^{\mu\nu} F_{\mu\nu}$ are not identical, despite having the same on-shell values (see Eq. (23)). The full energy-momentum tensor implied by Eq. (30) thus matches that implied by the original action given our assumptions.

notice in Eq. (30) that all $\chi(t)$ dependence has disappeared. This is because the ‘acceleration’ of the æther defined in Eq. (10) has only one non-vanishing component $J_r = d\mathcal{N}/dr$, whilst q^{tt} vanishes due to Eq. (22). The absence of $\chi(t)$ will be exploited in Section III B. From Eq. (30), the field equation associated with the one remaining scalar $\psi(r)$ takes the form of a conservation law

$$\nabla_\mu (J^\mu - (1 + \lambda_s) \nabla^\mu \psi) = 0, \quad (31)$$

which reflects the surviving shift symmetry.

Possible branches. — There are evidently at least two ways to realize Eq. (28), $\mathcal{Q}_0 = 0$ and $\mathcal{F}_{20} = 0$. Perhaps surprisingly, the $\mathcal{F}_{20}(\mathcal{Q} - \mathcal{Q}_0)^2$ term in Eq. (17) is absent from Eq. (30) not just in the case $\mathcal{F}_{20} = 0$ but also for $\mathcal{Q}_0 = 0$. This is because the condition $\mathcal{Q}_0 = 0$ is not only a statement about the constants parameterizing the action in Eq. (17), but also about the scalar field in Eq. (21). In particular, it eliminates all time dependence in φ , so that Eq. (23) leads to \mathcal{Q} vanishing identically, along with $\mathcal{F}_{20}(\mathcal{Q} - \mathcal{Q}_0)^2$. Despite the action in Eq. (30) having the same form for $\mathcal{F}_{20} = 0$ and $\mathcal{Q}_0 = 0$, the solutions in either case are not identical, as we will see below.

A. New branches of exact solutions

General case. — The first realisation of Eq. (28) will be through the condition

$$\mathcal{F}_{20} \neq 0, \quad \mathcal{Q}_0 = 0. \quad (32)$$

In this case, we satisfy Eq. (29) by assuming no time dependence in $\varphi(t, r)$, so that Eq. (21) implies simply

$$\chi(t) = 0. \quad (33)$$

The crucial point is that the reduced covariant action for $\mathcal{A}\mathcal{E}\mathcal{S}\mathcal{T}$ in Eq. (30) reduces to the corresponding action for $\mathcal{E}\mathcal{A}\mathcal{E}$ theory in Eq. (7) if $\nabla_\mu \psi$ is proportional to J_μ . For example, if

$$\nabla_\mu \psi = q J_\mu, \quad (34)$$

for some constant q , then Eq. (30) reduces to Eq. (7) in which K_B is replaced by an ‘effective’ æther coupling

$$K_B^{\text{eff}} \equiv K_B + (2 - K_B) q \left[2 - (1 + \lambda_s) q \right]. \quad (35)$$

This raises the possibility of ‘lifting’ solutions from the original $\mathcal{E}\mathcal{A}\mathcal{E}$ theory to $\mathcal{A}\mathcal{E}\mathcal{S}\mathcal{T}$. In component form, the condition in Eq. (34) implies

$$\frac{d\psi}{dr} = q \frac{d\mathcal{N}}{dr}, \quad (36)$$

but Eq. (36) is not the only condition on $\psi(r)$. It is shown in Appendix C that for static æther in static geometries

which solve the $\mathcal{E}\mathcal{A}\mathcal{E}$ field equations, one always has the identity

$$\nabla_\mu J^\mu = 0. \quad (37)$$

If Eq. (37) holds, then Eq. (31) requires that the scalar field must satisfy the massless Klein–Gordon equation

$$\nabla_\mu \nabla^\mu \psi = 0. \quad (38)$$

We reiterate that the reason for suppressing time dependence in Eq. (33) is that otherwise the heuristic action cannot reduce to $\mathcal{E}\mathcal{A}\mathcal{E}$ theory. By combining Eqs. (8) and (14) with Eq. (35) we obtain the physical range

$$2q \left[2 - (1 + \lambda_s) q \right] < K_B^{\text{eff}} < 2. \quad (39)$$

By comparing Eq. (8) with Eq. (39), we see how the upper bounds of K_B^{eff} and K_B are the same, whilst the ratio of the spatial gradient of the scalar to the æther acceleration in Eq. (34), and the parameter λ_s , alter the lower bound of K_B^{eff} .

Scalar hair. — Note that any choice of q other than $q = (1 + \lambda_s)^{-1}$ implies that there is a non-vanishing scalar current at spatial infinity. For that reason, such solutions were dismissed in [12] in the context of neutron stars. Indeed, such a constraint is required for consistency in the neutron star case, because the current flowing out at spatial infinity would otherwise not be balanced by any incoming current elsewhere (as required by charge conservation); the same holds for discussions of galaxies and galaxy clusters in $\mathcal{A}\mathcal{E}\mathcal{S}\mathcal{T}$ [10, 11, 58]. In our case, there *is* always a balancing current and all equations of motion can consistently be satisfied with a non-zero scalar current. Thus, in the following, we allow general values of q . That said, the balancing current often comes from regions where the spacetime is singular, so that the origin of these currents remains somewhat mysterious. For later reference, we record the value \bar{K}_B^{eff} following from Eq. (36) of K_B^{eff} for the case of no current at infinity, as¹⁴

$$\bar{K}_B^{\text{eff}} \equiv \frac{\lambda_s K_B + 2}{1 + \lambda_s}. \quad (40)$$

Unlike for a more general choice of q , the value in Eq. (40) is strictly positive. Thus, the GR limit $K_B^{\text{eff}} \rightarrow 0$ is only accessible when one allows a scalar current at infinity.

Ellis–Bronnikov drainhole. — In the (presumably non-physical) case where Eq. (8) is violated such that

$$K_B > 2, \quad (41)$$

the logic used in Eq. (39), shows that the ‘effective’ æther coupling also obeys

$$K_B^{\text{eff}} > 2. \quad (42)$$

¹⁴ Note that in [15] this corresponds precisely to $\bar{K}_B^{\text{eff}} \equiv 2\bar{n}$.

It is shown in Appendix D that the solutions in this case are Ellis–Bronnikov drainholes, such that the line element in Eq. (19) is constrained beyond Eq. (24) to

$$\mathcal{N}(r) = -\frac{2}{\sqrt{2K_B^{\text{eff}} - 4}} \cot^{-1} \left[\frac{2r}{G_N M \sqrt{2K_B^{\text{eff}} - 4}} \right], \quad (43a)$$

$$\mathcal{R}(r) = \frac{1}{\sqrt{2}} e^{-\mathcal{N}(r)} \sqrt{2r^2 + G_N^2 M^2 (K_B^{\text{eff}} - 2)}. \quad (43b)$$

In Eqs. (43a) and (43b) the constant M is the mass of the drainhole at spatial infinity.¹⁵ This spacetime has two asymmetric but asymptotically flat regions, and the embedding in Minkowski space is especially evident on the $r \rightarrow \infty$ side, whereupon $\mathcal{N}(r) \rightarrow 0$. From Eq. (43b) the radius of the throat, i.e. the minimum-area two-sphere, is found to be

$$\mathcal{R}_T = \sqrt{\frac{K_B^{\text{eff}}}{2}} G_N M \exp \left[\frac{\tan^{-1} \left(\sqrt{\frac{K_B^{\text{eff}}}{2} - 1} \right)}{\sqrt{\frac{K_B^{\text{eff}}}{2} - 1}} \right]. \quad (44)$$

As mentioned in Section II B, the geometry defined by Eqs. (19), (24), (43a) and (43b) also solves scalar-tensor theory in Eq. (6) in the phantom ‘(+)’ case.

First extended Eling–Jacobson solution. —

If Eq. (41) is not met, but rather K_B lies within the physical range of Eq. (8), then the solutions (see Appendix D) correspond to the Eling–Jacobson wormhole [66, 71, 72]. In this case Eqs. (43a) and (43b) are replaced by

$$\mathcal{N}(r) = \frac{\ln \left[1 - \sqrt{4 - 2K_B^{\text{eff}} \frac{G_N M}{r}} \right]}{\sqrt{4 - 2K_B^{\text{eff}}}}, \quad (45a)$$

$$\mathcal{R}(r) = r \left[1 - \sqrt{4 - 2K_B^{\text{eff}} \frac{G_N M}{r}} \right]^{\frac{1}{2} - \frac{1}{\sqrt{4 - 2K_B^{\text{eff}}}}}, \quad (45b)$$

and it may be shown that the asymptotically flat portion of Eqs. (19), (24), (45a) and (45b) corresponds to Eqs. (2) to (4) in different coordinates. Once again, M may be interpreted as the mass of the solution at spatial infinity $r \rightarrow \infty$, where asymptotic flatness again follows from $\mathcal{N}(r) \rightarrow 0$. From Eq. (45b) the formula for the throat radius given in Eq. (44) is now replaced by

$$\mathcal{R}_T = \sqrt{\frac{K_B^{\text{eff}}}{2}} G_N M \exp \left[\frac{\tanh^{-1} \left(\sqrt{1 - \frac{K_B^{\text{eff}}}{2}} \right)}{\sqrt{1 - \frac{K_B^{\text{eff}}}{2}}} \right]. \quad (46)$$

¹⁵ Note that M appears everywhere in combination with G_N . We have chosen it this way, in line with the expectation that the Newtonian limit of $\mathcal{A}EST$ be described by Eq. (16). Ultimately, however, M is an integration constant whose interpretation is flexible.

After passing through the throat, the volume element diverges as $r \rightarrow r_S$ from above, where

$$r_S \equiv 2G_N M \sqrt{1 - K_B^{\text{eff}}/2}. \quad (47)$$

It can be shown that this surface is a Killing horizon; in [66], it was also conjectured to be a null singularity. Moreover, this behavior is not uniquely seen in $E\mathcal{A}E$ theory or in $\mathcal{A}EST$. Instead, it seems to be a general phenomenon in other Lorentz-violating theories, such as bumblebee gravity [67]. Although it seems possible to extend the spacetime described by Eqs. (19), (24), (45a) and (45b) to the region $0 < r < r_S$ for certain values of K_B^{eff} , we prove in Appendix E that photon geodesics cannot be traced through the Killing horizon. As mentioned in Section II B, this geometry is best known as a solution to the $E\mathcal{A}E$ theory in Eq. (7) though — as we will see in Section III B — it is already known to occur in $\mathcal{A}EST$, albeit as part of a quite different solution branch to that considered here, in that the scalar is time-dependent [15].¹⁶

Anti-Ellis–Bronnikov solution. — We now relax the condition Eq. (34), and so lose the connection to $E\mathcal{A}E$ theory; as a consequence our results will no longer depend on K_B^{eff} . We impose the new condition

$$J^\mu = 0, \quad (48)$$

and it can be shown (see Appendix D) that Eqs. (45a) and (45b) are now replaced by

$$\mathcal{N}(r) = 0, \quad \mathcal{R}(r) = \sqrt{r^2 - \ell^2}, \quad (49)$$

where ℓ is an integration constant, whilst the condition in Eqs. (36) and (38) is replaced by

$$\psi(r) = \pm \frac{\sqrt{2} \tanh^{-1}(\ell/r)}{\sqrt{(2 - K_B)(1 + \lambda_s)}}. \quad (50)$$

To give an interpretation for ℓ , it follows from Eq. (49) that as $r \rightarrow |\ell|$ from above the scalar $\psi(r)$ will diverge. Thus, the geometry defined by Eqs. (19), (24) and (49) — which is evidently the ‘(–)’ configuration of that described in Eq. (5) — appears to describe a naked singularity. It is, moreover, *ultrastatic*, in stark contrast to the geometries in Eqs. (43a) and (45a). Indeed, in the cases of the Ellis–Bronnikov drainhole and the Eling–Jacobson wormhole, the redshift function $\mathcal{N}(r)$ has a non-trivial dependence on r . Parametrically, by keeping K_B^{eff} constant, the ultrastatic limit $\mathcal{N}(r) \rightarrow 0$ corresponds to the massless limit $M \rightarrow 0$ in both solutions — and in both solutions this limit is just Minkowski spacetime. As mentioned in Section II B, however, the Ellis–Bronnikov drainhole has another ultrastatic, massless

¹⁶ Note also that the $K_B^{\text{eff}} = 0$ (pure Schwarzschild) special case of Eqs. (45a) and (45b), with a truly static scalar as in our setup, was also identified in [15].

limit in which the throat \mathcal{R}_T is held constant in Eq. (44) through a simultaneous tuning of K_B^{eff} . The resulting symmetric wormhole is precisely described by the geometry in Eq. (49) under the analytic continuation

$$\ell \mapsto i\ell, \quad (51)$$

— i.e. the ‘(+)’ configuration of Eq. (5) — and for this reason we refer to Eq. (49) as ‘anti-Ellis–Bronnikov’ spacetime. Whilst the geometry remains real under this analytic continuation, by tracing Eq. (51) through Eq. (50) we find that the scalar field $\psi(r)$ becomes imaginary. It is natural, therefore, to conjecture that anti-Ellis–Bronnikov spacetime is an exact solution to the scalar-tensor theory in Eq. (6) in the canonical ‘(–)’ case. Referring back to our discussion in Section II B, this would suggest that it corresponds to an ultrastatic limit of Fisher–JNW spacetime.

B. Connection to previous branches

Second extended Eiling–Jacobson solution.

We now enforce Eq. (28) through the condition complementary to that given in Eq. (32), namely

$$\mathcal{F}_{20} = 0, \quad \mathcal{Q}_0 \neq 0. \quad (52)$$

The scenario in Eq. (52) was considered in [15], where Eq. (33) is replaced by assuming a linear time dependence of the scalar

$$\chi(t) = t. \quad (53)$$

The motivation for Eq. (53) is that it matches the expected late-time cosmological behavior for the scenario envisioned originally in [10]. Here, we point out that a more general solution is possible, with an *arbitrary* time dependence of the scalar replacing Eq. (53). That this is possible may be expected from the fact that the existence of a time-dependent $\chi(t)$ scalar field does not modify the heuristic action in Eq. (30). Due to the time dependence in the scalar, the constraint Eq. (29) now becomes non-trivial, since the overall prefactor $d\chi/dt$ no longer vanishes. In fact, the constraint now requires that the conserved current associated with the scalar’s shift symmetry (see Eq. (31)) vanishes identically according to

$$J^\mu - (1 + \lambda_s) \nabla^\mu \psi = 0. \quad (54)$$

The on-shell condition in Eq. (54) may be viewed as a special case of Eq. (34), namely

$$q = (1 + \lambda_s)^{-1}. \quad (55)$$

With Eq. (55) satisfied, all the results of Section III A now apply here. In particular, and assuming the physical range in Eq. (8), the metric is that of Eqs. (45a)

and (45b), but restricted to the case where \bar{K}_B^{eff} is the value of K_B^{eff} for our particular choice of q (see Eq. (40))

$$\mathcal{N}(r) = \frac{\ln \left[1 - \sqrt{4 - 2\bar{K}_B^{\text{eff}} \frac{G_N M}{r}} \right]}{\sqrt{4 - 2\bar{K}_B^{\text{eff}}}}, \quad (56a)$$

$$\mathcal{R}(r) = r \left[1 - \sqrt{4 - 2\bar{K}_B^{\text{eff}} \frac{G_N M}{r}} \right]^{\frac{1}{2} - \frac{1}{\sqrt{4 - 2\bar{K}_B^{\text{eff}}}}}, \quad (56b)$$

and the geometry defined by Eqs. (19), (24), (56a) and (56b) matches the corresponding metric from [15]. According to Eq. (21), the scalar is given by

$$\psi(r) = (1 + \lambda_s)^{-1} \mathcal{N}(r) + \text{const.} \quad (57)$$

Since the spacetime geometry is expected to dictate most of the observables in the strong-field regime, it is especially interesting to notice how the BH mimicker geometry arises across multiple field configurations for the scalar. Finally, we reiterate the differences between the first and second extended Eiling–Jacobson solutions, and the way in which they extend the solutions already presented in [15]. The first extended solution follows from a truly static scalar field, and allows for an ‘effective’ æther coupling as defined in Eq. (35), depending only on the static profile of the scalar. The second extended solution allows for a scalar with completely arbitrary time-dependence $\chi(t)$: it also gives rise to an ‘effective’ æther coupling, but this coupling is *not* derived from Eq. (35), and is instead fixed to the special value in Eq. (40) as a consequence of $q = (1 + \lambda_s)^{-1}$. The special case of the first extended solution in which $K_B^{\text{eff}} = 0$ was identified in [15]. The special case of the second extended solution, in which $\chi(t) = t$, was also identified in [15].

IV COSMOLOGICAL CASE

Einstein static universe. — Before concluding (and mostly for completeness), we discuss a cosmological solution that admits a purely timelike æther field. While not asymptotically flat, this provides a contrast to the isolated solutions of Section III and connects to the large-scale phenomenology of the theory. We relax the conditions in Eqs. (26) and (28), and so re-admit the CDM component to the ÆST action. Introducing a new constant Λ of mass dimension four, the conditions in Eqs. (19) and (24) are extended (see Appendix D) by

$$\mathcal{N}(r) = 0, \quad \mathcal{R}(r) = \frac{\sin(\sqrt{\kappa\Lambda}r)}{\sqrt{\kappa\Lambda}}, \quad (58)$$

and from Eq. (58) we see that Eq. (25) can be satisfied by precisely the linear running condition in Eq. (53). Evidently, the spacetime geometry described by Eqs. (19), (24) and (58) corresponds to the Einstein static universe, i.e., a solution of the Einstein equations with dust (or

CDM) and a cosmological constant Λ . With reference to Eq. (17), it is not therefore surprising that other field equations require Eq. (26) to be replaced by

$$\mathcal{V}(\mathcal{Y}) = 2\kappa\Lambda. \quad (59)$$

Accordingly, this solution is valid only when the parameters of $\mathcal{A}\mathcal{E}\mathcal{S}\mathcal{T}$ are carefully chosen to support Eq. (59). For other choices of the coupling parameters, the æther must not be purely timelike. The field $\psi(r)$ is meanwhile given by

$$\psi(r) = -\frac{\sqrt{\kappa\Lambda}r \cot(\sqrt{\kappa\Lambda}r)}{(2 - K_B)}. \quad (60)$$

Although the spacetime in Eqs. (19), (24) and (58) is homogeneous, this property is not shared by the scalar field in Eq. (60).

V CONCLUSIONS

Summary. — Because æther-scalar-tensor theory provides modified Newtonian dynamics, there is (somewhat unusually) no incentive to interpret the exotic compact objects found above as dark matter candidates. For the reasons given in Section I, we identify the Eling–Jacobson-type solutions as *black hole mimickers*, and the anti-Ellis–Bronnikov solutions as *Shapiro-free lenses*. Respectively, we imagine these as secretly accounting for some fraction of the apparently observed black hole population, and as a quiet source of anomalous lensing events. The question of production, stability and detection of these objects is left for future work.

Formal æther-scalar-tensor results. — We have obtained several spherically symmetric exact solutions to the æther-scalar-tensor theory of gravity with static spacetime geometry, and an æther field which is aligned with the timelike Killing vector. When the modified Newtonian dynamics and effective cold dark matter sectors are neglected (as may be expected in the strong-field regime) we find three branches of asymptotically flat solutions:

- If the gradient of the scalar is static, and is aligned with the æther acceleration, there is an exact correspondence with Einstein-æther theory in which the æther coupling is renormalised by the scalar flux at infinity. For stable values of the bare æther coupling, this correspondence leads to the famous Eling–Jacobson wormhole; an unstable æther coupling leads to an Ellis–Bronnikov drainhole.
- Alternatively, if the scalar is static but the æther has no acceleration, then the Einstein-æther correspondence is broken. This leads to the line element of anti-Ellis–Bronnikov spacetime. In real terms, static observers in this geometry feel no acceleration, but there is a naked scalar singularity.

- The Eling–Jacobson solution also reappears when the scalar rolls linearly in time (as motivated by the requirements of cosmology), and this scenario may be extended to arbitrary time dependence of the scalar.
- When the cold dark matter sector is included, along with a cosmological constant, a non-asymptotically-flat solution is found, which has the same spacetime geometry as the Einstein static universe. This geometry is homogeneous, but the scalar field exhibits a profile, introducing a preferred centre.

Formal Einstein-æther results. — The Einstein-æther correspondence also leads us to obtain several formal results in that theory. Firstly, we confirm previous conjectures that Eling–Jacobson spacetime is inextendible beyond the Killing horizon on the ‘interior’ of the throat, which is shown to be a null singularity. This result may be relevant to bumblebee gravity [67], which features solutions very similar to the Eling–Jacobson wormhole. Secondly, we show that when the æther field is aligned with a timelike Killing vector field, the æther acceleration is always a conserved current.

Why scalar hair is allowed. — One possible objection to the new solutions is that they are hairy: they emit a flux of the conserved current associated with the shift symmetry of the scalar: the model — being completely shift-symmetric — seemingly provides no charge to source this flux. This objection can be disregarded, because æther-scalar-tensor theory is formulated in the context of cosmology and astrophysics on large scales. Once the theory is quantised there is a generic expectation that symmetry-breaking operators will be introduced at the one-loop level. This runs contrary to notable counterexamples of relevance to no-hair theorems: in Galileon/Horndeski theory, the derivative interactions are such that loops from Galileon vertices never generate lower-derivative symmetry-breaking operators. More generally, however, coupling of shift-symmetric scalars to matter or gravity *is* expected to result in symmetry breaking. This effect would need to be taken into account when matching our solutions to extreme matter configurations. Indeed, despite our observations that both the black hole mimicker and the Shapiro-free lens solutions terminate at singular regions, there is no obvious reason why exotic matter sources cannot be introduced to avoid this. Such an attempt seems particularly desirable in the case of the lens, which would otherwise have a naked singularity, though the non-self-gravitating nature of the solution may give rise to particular challenges. In either case, hair may be sourced by quantum corrections that arise in the extreme environments on the approach to singular regions, where all current models eventually break down.

Observational outlook: mimickers. — From an observational perspective, such æther-inspired com-

compact objects could produce distinctive signatures in upcoming surveys and multi-messenger data. For example, mergers of black hole mimickers might display non-standard gravitational wave ringdown: several studies predict late-time echoes or ‘anti-chirps’ rather than the standard Kerr quasinormal modes [25, 73]. Detecting these subtle signals will require the high sensitivity of LIGO/Virgo/KAGRA’s O4 run and next-generation observatories (Einstein Telescope, Cosmic Explorer), and space-based missions such as LISA could also probe extreme-mass-ratio inspirals around super-

massive mimickers. Moreover, if horizons are absent, infalling matter could emit prompt electromagnetic or neutrino bursts, making coordinated gravitational/electromagnetic/neutrino searches (e.g. IceCube, Fermi/Swift) a promising avenue. At the most basic level, we provide the rudimentary formulae corresponding to the radii (in the Schwarzschild-like coordinates of Eq. (2)) corresponding to the photon sphere r_γ and the innermost stable circular orbit r_{ISCO} , for the mimicker proposed in Eqs. (2) to (4). These formulae, which are used to obtain the slightly dilated radii illustrated in Fig. 1, are respectively

$$r_\gamma \equiv G_N M \sqrt{3 + \frac{K_B^{\text{eff}}}{2}} \left[\left(\frac{\sqrt{2} + \sqrt{2 - K_B^{\text{eff}}}}{\sqrt{2} - \sqrt{2 - K_B^{\text{eff}}}} \right) \left(\frac{2 + K_B^{\text{eff}} - \sqrt{2}\sqrt{2 - K_B^{\text{eff}}}}{2 + K_B^{\text{eff}} + \sqrt{2}\sqrt{2 - K_B^{\text{eff}}}} \right) \right]^{\frac{1}{\sqrt{4 - 2K_B^{\text{eff}}}}}, \quad (61a)$$

$$r_{\text{ISCO}} \equiv \frac{G_N M \sqrt{K_B^{\text{eff}}} \sqrt{4 + K_B^{\text{eff}} - \sqrt{2}\sqrt{8 + K_B^{\text{eff}}}}}{\sqrt{10 + K_B^{\text{eff}} - 2\sqrt{2}\sqrt{8 + K_B^{\text{eff}}} - \sqrt{2}}} \left[\left(\frac{\sqrt{2} + \sqrt{2 - K_B^{\text{eff}}}}{\sqrt{2} - \sqrt{2 - K_B^{\text{eff}}}} \right) \times \left(\frac{\sqrt{10 + K_B^{\text{eff}} - 2\sqrt{2}\sqrt{8 + K_B^{\text{eff}}} - \sqrt{2 - K_B^{\text{eff}}}}}{\sqrt{10 + K_B^{\text{eff}} - 2\sqrt{2}\sqrt{8 + K_B^{\text{eff}}} + \sqrt{2 - K_B^{\text{eff}}}}} \right) \right]^{\frac{1}{\sqrt{4 - 2K_B^{\text{eff}}}}}. \quad (61b)$$

To reiterate the physical parameters, besides the Newtonian mass M , the formulae in Eqs. (61a) and (61b) refer to the measured Newton–Cavendish constant G_N as defined in Eq. (16), and the dimensionless number K_B^{eff} as defined in Eq. (35), with particular physical significance granted the ‘special’ value \bar{K}_B^{eff} as defined in Eq. (40). A possible objection to the possibility that some observed black holes may be mimickers is that the accreting matter is not hidden behind an infinite-redshift horizon. Indeed, if matter were to ‘loiter’ at the throat, it may give rise to observable X-ray emissions. To address this, we note that the throat is guaranteed to be an unstable environment for orbiting matter, since it always lies well within the ISCO. To address this question more broadly, we provide the formula for the proper acceleration experienced by massive, static observers at the wormhole throat:¹⁷

$$|\mathbf{a}| = \frac{2(2 - K_B^{\text{eff}})}{G_N M K_B^{\text{eff}}} \left(\frac{\sqrt{2} - \sqrt{2 - K_B^{\text{eff}}}}{\sqrt{2} + \sqrt{2 - K_B^{\text{eff}}}} \right)^{\frac{1}{\sqrt{4 - 2K_B^{\text{eff}}}}}. \quad (62)$$

The important point is that Eq. (62) approaches zero in the extremal case $K_B^{\text{eff}} \rightarrow 2$, and diverges in the ‘stealth’ limit of GR as $K_B^{\text{eff}} \rightarrow 0$. For all finite values of K_B^{eff} , however, matter loitering at the throat would need to be sustained by an outward acceleration of $|\mathbf{a}| \sim 1/G_N M$. In the case of a solar-mass mimicker, this is comparable to the surface gravity of a neutron star at $|\mathbf{a}| \sim 6 \times 10^{13} \text{ m s}^{-2}$. For a supermassive mimicker, the acceleration may be suppressed by a factor of 10^{6-9} . For much of the parameter space, therefore, it is reasonable to expect that mimicker throats would not be visible, though for large masses and extremal values of K_B^{eff} , observable signatures may be expected and should be investigated.

Observational outlook: lenses. — Meanwhile, Shapiro-free (massless) lenses may behave like cosmic strings: multiple images with identical magnification and essentially zero Shapiro time delay. Indeed, to leading order, the Shapiro time delay in the weak-field limit is

$$\Delta t \approx -b \frac{\ell^2}{2b^2} \left[\arccos\left(\frac{b}{r_s}\right) + \arccos\left(\frac{b}{r_o}\right) \right], \quad (63)$$

where b is the impact parameter, r_s is the coordinate distance of the source to the singularity and r_o the distance of the observer. By contrast the GR expression, com-

¹⁷ Note that for the non-physical case $K_B^{\text{eff}} > 2$ we would have $|\mathbf{a}| = 2 \exp \left[-\tan^{-1} \left(2/\sqrt{-4 + 2K_B^{\text{eff}}} \right) / \sqrt{-4 + 2K_B^{\text{eff}}} \right] / (G_N M K_B^{\text{eff}})$ in place of Eq. (62).

puted from the Schwarzschild line element in Eq. (1), is

$$\Delta t \approx 2b \frac{GM}{b} \left[1 + \ln \left(\frac{4r_o r_s}{b^2} \right) \right]. \quad (64)$$

When we compare Eq. (63) with Eq. (64), we notice that the former has the opposite sign and, more importantly, does not diverge for far away observers or far away sources. Indeed, in the limit $r_o \rightarrow \infty$ and $r_s \rightarrow \infty$, the exact expression for the time delay, not assuming the weak-field limit, converges to

$$\Delta t = 2b \left[K \left(-\frac{\ell^2}{b^2} \right) - E \left(-\frac{\ell^2}{b^2} \right) \right], \quad (65)$$

where K and E are the complete elliptic integrals of the first and second kind, respectively. Thus, for typical astrophysical and cosmological scales, we expect these lenses to be practically Shapiro-less. Regarding the sign of Eq. (63), implying a Shapiro advance rather than a delay, we note that this phenomenology is likely not unique to the Shapiro-less lenses discussed here. Indeed, the gravitational acceleration around galaxies and galaxy clusters in æther-scalar-tensor theory is expected to oscillate at very large radii [10, 11, 58]. This corresponds to an oscillating effective mass profile that would, in some regions, likely induce a Shapiro advance. The implications and phenomenology of these negative Shapiro delays in æther-scalar-tensor theory will be investigated in future work. Note that, whilst we focus on the Shapiro time delay in this work, other lensing characteristics are comparably reduced and inverted. Working again at the most basic level, the ‘(−)’ configuration of Eq. (5), which describes the lens, can be used to compute the effective Weyl potential relevant to gravitational lensing $\Phi_{\text{lens}} \equiv (\Phi_N + \Psi_N)/2$ in the Newtonian limit $ds^2 \approx -(1 + 2\Phi_N)dt^2 + (1 - 2\Psi_N)(dr^2 + r^2 d\Omega^2)$.¹⁸ We find that ultrastaticity of the lens leads to a vanishing redshift potential $\Phi_N = 0$, such that to leading order in ℓ/r

$$\Phi_{\text{lens}} = \frac{1}{2}\Psi_N \approx \frac{\ell^2}{8r^2}. \quad (66)$$

Note once again that Eq. (66) contrasts strongly in terms of sign and scaling with the GR case, computed from the Schwarzschild line element in Eq. (1), for which $\Phi_{\text{lens}} = \Phi_N = \Psi_N = -G_N M/r$. Indeed, if one were to interpret the lensing signal implied by Eq. (66) in terms of a non-relativistic matter source in GR, one would infer a mass profile

$$M(r) \approx -\frac{\ell^2}{4G_N r}. \quad (67)$$

¹⁸ Note that the conventional line element for weak-field lensing calculations corresponds to a choice of *isotropic* coordinates, which differ from the Schwarzschild coordinates in Eq. (1) and proper-radial coordinates in Eq. (5) by some rescaling of the radii.

Evidently, the profile in Eq. (67) is grossly anomalous. It corresponds to a compact negative mass surrounded (and exactly cancelled) by a diffuse positive $\sim 1/r^4$ density profile, such as those used to model the stellar mass density in elliptical galaxies and bulges [74–76] (see also [77]). Such an object would not be physical in the GR context, but it could be explained by æther-scalar-tensor theory without recourse to exotic matter of any kind. Extending the approximations in Eqs. (66) and (67), the exact lensing deflection angle $\Delta\phi$, not assuming the weak-field limit, is given by

$$\Delta\phi = 2K \left(-\frac{\ell^2}{b^2} \right) - \pi, \quad (68)$$

where b is the impact parameter and K is once again the complete elliptical integral of the first kind. Time-domain instruments such as the Rubin Observatory (LSST) and Roman Space Telescope, together with radio facilities (SKA, CHIME), will monitor large numbers of transients and strongly lensed systems. These campaigns can test for anomalous lensing. Strongly lensed gravitational wave signals could exhibit interference fringes or multiple chirps with unexpected timing. In summary, a coordinated multi-messenger strategy is key: gravitational wave detectors (O4 and beyond) searching for non-GR ringdowns, alongside precise timing and imaging surveys for synchronized lensing transients, may constrain or reveal these phenomena. The advent of SKA, LSST/Rubin, Roman, LISA and IceCube thus provides concrete opportunities towards a smoking gun for æther-scalar-tensor black hole mimickers and Shapiro-free lenses.

ACKNOWLEDGMENTS

This work was improved by many useful discussions with Justin Feng, Mike Hobson, Yi-Hsiung Hsu, Ted Jacobson, Anthony Lasenby, Constantinos Skordis, David Vokrouhlický, Jingbo Yang and Tom Złosnik.

This work used the DiRAC Data Intensive service (CSD3 www.csd3.cam.ac.uk) at the University of Cambridge, managed by the University of Cambridge University Information Services on behalf of the STFC DiRAC HPC Facility (www.dirac.ac.uk). The DiRAC component of CSD3 at Cambridge was funded by BEIS, UKRI and STFC capital funding and STFC operations grants. DiRAC is part of the UKRI Digital Research Infrastructure.

This work also used the Newton server, access to which was provisioned by Will Handley using an ERC grant.

WB is grateful for the support of Girton College, Cambridge, Marie Skłodowska-Curie Actions and the Institute of Physics of the Czech Academy of Sciences. AD was supported by the European Regional Development Fund and the Czech Ministry of Education, Youth and Sports: project MSCA Fellowship CZ FZU I —

CZ.02.01.01/00/22_010/0002906. TM was supported by the DFG (German Research Foundation) – 514562826.

Co-funded by the European Union. Views and opinions expressed are however those of the author(s) only

and do not necessarily reflect those of the European Union or European Research Executive Agency. Neither the European Union nor the granting authority can be held responsible for them.

-
- [1] S. S. McGaugh, J. M. Schombert, G. D. Bothun, and W. J. G. de Blok, *Astrophys. J. Lett.* **533**, L99 (2000), [arXiv:astro-ph/0003001 \[astro-ph\]](#).
 - [2] T. Mistele, S. McGaugh, F. Lelli, J. Schombert, and P. Li, *Astrophys. J. Lett.* **969**, L3 (2024), [arXiv:2406.09685 \[astro-ph.GA\]](#).
 - [3] T. Mistele, *Phys. Rev. D* **110**, 024062 (2024), [arXiv:2305.07742 \[gr-qc\]](#).
 - [4] M. M. Brouwer, K. A. Oman, E. A. Valentijn, M. Bilicki, C. Heymans, H. Hoekstra, N. R. Napolitano, N. Roy, C. Tortora, A. H. Wright, M. Asgari, J. L. van den Busch, A. Dvornik, T. Erben, B. Giblin, A. W. Graham, H. Hildebrandt, A. M. Hopkins, A. Kannawadi, K. Kuijken, J. Liske, H. Shan, T. Tröster, E. Verlinde, and M. Visser, *Astronomy & Astrophysics* **650**, A113 (2021), [arXiv:2106.11677 \[astro-ph.GA\]](#).
 - [5] F. Lelli, S. S. McGaugh, J. M. Schombert, and M. S. Pawlowski, *Astrophys. J.* **836**, 152 (2017), [arXiv:1610.08981 \[astro-ph.GA\]](#).
 - [6] M. Milgrom, *Astrophys. J.* **270**, 365 (1983).
 - [7] M. Milgrom, *Astrophys. J.* **270**, 371 (1983).
 - [8] M. Milgrom, *Astrophys. J.* **270**, 384 (1983).
 - [9] B. Famaey and S. McGaugh, *Living Rev. Rel.* **15**, 10 (2012), [arXiv:1112.3960 \[astro-ph.CO\]](#).
 - [10] C. Skordis and T. Zlosnik, *Phys. Rev. Lett.* **127**, 161302 (2021), [arXiv:2007.00082 \[astro-ph.CO\]](#).
 - [11] T. Mistele, S. McGaugh, and S. Hossenfelder, *Astronomy & Astrophysics* **676**, A100 (2023), [arXiv:2301.03499 \[astro-ph.GA\]](#).
 - [12] C. Reyes and J. Sakstein, *Phys. Rev. D* **110**, 084019 (2024), [arXiv:2406.18225 \[gr-qc\]](#).
 - [13] C. Reyes and J. Sakstein, *arXiv preprints* (2025), [arXiv:2505.03527 \[gr-qc\]](#).
 - [14] R. C. Bernardo and C.-Y. Chen, *General Relativity and Gravitation* **55**, 10.1007/s10714-023-03075-x (2023).
 - [15] C. Skordis and D. M. J. Vokrouhlicky, *JCAP* **03**, 035, [arXiv:2412.15395 \[gr-qc\]](#).
 - [16] C. T. Bolton, *Nature* **235**, 271 (1972).
 - [17] R. A. Remillard and J. E. McClintock, *Annu. Rev. Astron. Astrophys.* **44**, 49 (2006).
 - [18] R. Schödel, T. Ott, R. Genzel, A. Eckart, N. Mouawad, and T. Alexander, *Nature* **419**, 694 (2002).
 - [19] A. M. Ghez, S. Salim, N. N. Weinberg, and et al., *Astrophys. J.* **689**, 1044 (2008).
 - [20] D. Lynden-Bell and M. J. Rees, *Mon. Not. Roy. Astron. Soc.* **152**, 461 (1971).
 - [21] J. Kormendy and L. C. Ho, *Annu. Rev. Astron. Astrophys.* **51**, 511 (2013).
 - [22] R. Narayan and J. S. Heyl, *Astrophys. J.* **574**, L139 (2002).
 - [23] R. Narayan and J. E. McClintock, *New Astron. Rev.* **51**, 733 (2008).
 - [24] B. Abbott, R. Abbott, T. Abbott, e. L. S. Collaboration, and V. Collaboration), *Phys. Rev. Lett.* **116**, 221101 (2016).
 - [25] V. Cardoso, E. Franzin, and P. Pani, *Phys. Rev. Lett.* **116**, 171101 (2016).
 - [26] H. Falcke, F. Melia, and E. Agol, *Astrophys. J. Lett.* **528**, L13 (2000).
 - [27] K. e. Event Horizon Telescope Collaboration; Akiyama, *Astrophys. J. Lett.* **875**, L1 (2019).
 - [28] K. e. Event Horizon Telescope Collaboration; Akiyama, *Astrophys. J. Lett.* **930**, L12 (2022).
 - [29] Y. Tanaka, K. Nandra, A. C. Fabian, and et al., *Nature* **375**, 659 (1995).
 - [30] A. C. Fabian, K. Iwasawa, C. S. Reynolds, and A. J. Young, *Publ. Astron. Soc. Pac.* **112**, 1145 (2000).
 - [31] R. e. GRAVITY Collaboration (Abuter, *Astron. Astrophys.* **615**, L15 (2018).
 - [32] R. e. GRAVITY Collaboration (Abuter, *Astron. Astrophys.* **636**, L5 (2020).
 - [33] I. Gott, J. Richard, *Astrophysical Journal* **288**, 422 (1985).
 - [34] D. Huterer and T. Vachaspati, *Physical Review D* **68**, 041301 (2003).
 - [35] P. Tisserand, L. Le Guillou, C. Afonso, and et al., *Astronomy & Astrophysics* **469**, 387 (2007).
 - [36] P. Mróz, A. Udalski, M. K. Szymański, L. Wyrzykowski, and et al., *Astrophysical Journal Supplement* **273**, 4 (2024).
 - [37] K. T. Inoue, *New Astronomy* **58**, 47 (2018).
 - [38] H. Niikura, M. Takada, N. Yasuda, R. H. Lupton, T. Sumi, S. More, T. Kurita, S. Sugiyama, A. More, M. Oguri, and M. Chiba, *Nature Astronomy* **3**, 524 (2019).
 - [39] J. H. Taylor and J. M. Weisberg, *Astrophysical Journal* **345**, 434 (1989).
 - [40] M. Kramer, I. H. Stairs, R. N. Manchester, N. Wex, and et al., *Physical Review X* **11**, 041050 (2021).
 - [41] K. Lazaridis, N. Wex, A. Jessner, M. Kramer, B. W. Stappers, J. P. W. Verbiest, T. M. Tauris, and et al., *Monthly Notices of the Royal Astronomical Society* **400**, 805 (2009).
 - [42] P. C. C. Freire, N. Wex, G. Esposito-Farèse, J. P. W. Verbiest, M. Bailes, M. Kramer, I. H. Stairs, J. Antoniadis, and G. H. Janssen, *Monthly Notices of the Royal Astronomical Society* **423**, 3328 (2012).
 - [43] G. Agazie, Z. Arzoumanian, P. T. Baker, B. Bécsy, and et al., *Astrophysical Journal Letters* **951**, L8 (2023).
 - [44] J. Antoniadis, M. Bailes, P. Brem, and et al., *Astronomy & Astrophysics* **678**, A50 (2023).
 - [45] H. G. Ellis, *Journal of Mathematical Physics* **14**, 104 (1973).
 - [46] K. A. Bronnikov, *Acta Physica Polonica B* **4**, 251 (1973).
 - [47] M. Visser, *Nuclear Physics B* **328**, 203 (1989).
 - [48] M. Visser, *Lorentzian Wormholes: From Einstein to Hawking* (AIP Press, New York, 1995).
 - [49] M. S. Morris and K. S. Thorne, *American Journal of Physics* **56**, 395 (1988).

- [50] M. S. Morris, K. S. Thorne, and U. Yurtsever, *Physical Review Letters* **61**, 1446 (1988).
- [51] S. Sonogo, *Journal of Mathematical Physics* **51**, 092502 (2010).
- [52] I. I. Shapiro, *Physical Review Letters* **13**, 789 (1964).
- [53] I. I. Shapiro, G. H. Pettengill, M. E. Ash, M. L. Stone, W. B. Smith, R. P. Ingalls, and R. A. Brockelman, *Physical Review Letters* **20**, 1265 (1968).
- [54] C. Skordis and T. Zlosnik, *Phys. Rev. D* **106**, 104041 (2022), [arXiv:2109.13287 \[gr-qc\]](#).
- [55] T. Jacobson and D. Mattingly, *Physical Review D* **64**, 10.1103/physrevd.64.024028 (2001).
- [56] C. Eling, T. Jacobson, and D. Mattingly, Einstein-aether theory (2005), [arXiv:gr-qc/0410001 \[gr-qc\]](#).
- [57] C. Skordis and T. Zlosnik, *Phys. Rev. D* **106**, 104041 (2022).
- [58] A. Durakovic and C. Skordis, *JCAP* **04**, 040, [arXiv:2312.00889 \[astro-ph.CO\]](#).
- [59] H. Huang, H. Lü, and J. Yang, *Classical and Quantum Gravity* **39**, 185009 (2022).
- [60] S. Yazadjiev, *Phys. Rev. D* **96**, 044045 (2017).
- [61] H. G. Ellis, *Gen. Rel. Grav.* **10**, 105 (1979).
- [62] W.-J. Geng and H. Lü, *Phys. Rev. D* **93**, 044035 (2016).
- [63] H. Huang, J. Kunz, J. Yang, and C. Zhang, *Phys. Rev. D* **107**, 104060 (2023).
- [64] I. Z. Fisher, *Zh. Eksp. Teor. Fiz.* **18**, 636 (1948).
- [65] A. I. Janis, E. T. Newman, and J. Winicour, *Physical Review Letters* **20**, 878 (1968).
- [66] C. Eling and T. Jacobson, *Classical and Quantum Gravity* **23**, 5643 (2006).
- [67] R. Xu, D. Liang, and L. Shao, *Phys. Rev. D* **107**, 024011 (2023).
- [68] Y.-H. Hsu, A. Lasenby, W. Barker, A. Durakovic, and M. Hobson, *arXiv e-Prints* (2024), [arXiv:2411.02550 \[gr-qc\]](#).
- [69] R. Palais, *Communications in Mathematical Physics* **69**, 19 (1979).
- [70] M. E. Fels and C. G. Torre, *Classical and Quantum Gravity* **19**, 641–675 (2002).
- [71] J. Oost, S. Mukohyama, and A. Wang, *Universe* **7**, 272 (2021).
- [72] C. Gao and Y.-G. Shen, *Physical Review D* **88**, 10.1103/physrevd.88.103508 (2013).
- [73] S.-s. Bao, S. Hou, and H. Zhang, *Eur. Phys. J. C* **83**, 127 (2023).
- [74] W. Jaffe, *Monthly Notices of the Royal Astronomical Society* **202**, 995 (1983).
- [75] L. Hernquist, *The Astrophysical Journal* **356**, 359 (1990).
- [76] W. Dehnen, *Monthly Notices of the Royal Astronomical Society* **265**, 250 (1993).
- [77] A. Kassiola and I. Kovner, *The Astrophysical Journal* **417**, 450 (1993).
- [78] C. Eling, T. Jacobson, and M. C. Miller, *Physical Review D* **76**, 042003 (2007).

A DETAILS OF COVARIANT EQUATIONS

Definitions. — In this appendix, we present the covariant field equations extracted from the action Eq. (9), which we here write as

$$S_{\text{ÆST}} \equiv \int d^4x \frac{\sqrt{-g}}{2\kappa} \left[R - \frac{K_B}{2} F^{\mu\nu} F_{\mu\nu} + b J^\mu \nabla_\mu \varphi - \mathcal{G}(\mathcal{Y}, \mathcal{Q}) - \lambda (A^\mu A_\mu + 1) \right], \quad (\text{A1})$$

where we define the quantities

$$\mathcal{G}(\mathcal{Y}, \mathcal{Q}) \equiv (2 - K_B) \mathcal{Y} + \mathcal{F}(\mathcal{Y}, \mathcal{Q}), \quad a \equiv \frac{b}{2}(1 + \lambda_s), \quad b \equiv 2(2 - K_B). \quad (\text{A2})$$

The shorthand a does not appear explicitly in this form of the action but will be useful below. Unlike in Eq. (17), which assumes the specific form Eq. (11) of the function $\mathcal{F}(\mathcal{Y}, \mathcal{Q})$, here we do not make any such assumptions.

Equations. — The equations for the vector A_μ , the scalar φ , and the metric $g_{\mu\nu}$ obtained from Eq. (A1) are:

$$\begin{aligned} \frac{\delta S_{\text{ÆST}}}{\delta A_\mu} &\propto -2\lambda A^\mu + b(\nabla^\mu A^\nu)(\nabla_\nu \varphi) - 2K_B(\nabla_\nu \nabla^\mu A^\nu) - bA^\nu(\nabla_\nu \nabla^\mu \varphi) + 2K_B(\nabla_\nu \nabla^\nu A^\mu) \\ &\quad - (\nabla^\mu \varphi) \left(b(\nabla_\nu A^\nu) + \mathcal{G}^{(0,1)} + 2A^\nu(\nabla_\nu \varphi) \left(2 - K_B + \mathcal{G}^{(1,0)} \right) \right) = 0, \end{aligned} \quad (\text{A3a})$$

$$\begin{aligned} \frac{\delta S_{\text{ÆST}}}{\delta \varphi} &\propto -bA^\mu(\nabla_\nu \nabla_\mu A^\nu) - b(\nabla_\mu A_\nu)(\nabla^\nu A^\mu) + (\nabla_\mu A^\mu) \mathcal{G}^{(0,1)} + A^\mu(\nabla_\mu A^\nu)(\nabla_\nu \varphi) \mathcal{G}^{(0,2)} + A^\mu A^\nu(\nabla_\nu \nabla_\mu \varphi) \mathcal{G}^{(0,2)} \\ &\quad + 2(\nabla_\mu \nabla^\mu \varphi) \mathcal{G}^{(1,0)} + 2A^\mu(\nabla_\mu \varphi)(\nabla_\nu A^\nu) \mathcal{G}^{(1,0)} + 2A^\mu(\nabla_\mu A^\nu)(\nabla_\nu \varphi) \mathcal{G}^{(1,0)} + 2A^\mu A^\nu(\nabla_\nu \nabla_\mu \varphi) \mathcal{G}^{(1,0)} \\ &\quad + 2(\nabla_\mu \varphi)(\nabla_\nu \varphi)(\nabla^\nu A^\mu) \mathcal{G}^{(1,1)} + 2A^\mu(\nabla_\mu \nabla_\nu \varphi)(\nabla^\nu \varphi) \mathcal{G}^{(1,1)} + 2A^\mu(\nabla_\nu \nabla_\mu \varphi)(\nabla^\nu \varphi) \mathcal{G}^{(1,1)} \\ &\quad + 4A^\mu A^\nu(\nabla_\mu A^\rho)(\nabla_\nu \varphi)(\nabla_\rho \varphi) \mathcal{G}^{(1,1)} + 4A^\mu A^\nu A^\rho(\nabla_\mu \varphi)(\nabla_\rho \nabla_\nu \varphi) \mathcal{G}^{(1,1)} + 4(\nabla^\mu \varphi)(\nabla_\nu \nabla_\mu \varphi)(\nabla^\nu \varphi) \mathcal{G}^{(2,0)} \\ &\quad + 4A^\mu A^\nu A^\rho(\nabla_\mu A^\sigma)(\nabla_\nu \varphi)(\nabla_\rho \varphi)(\nabla_\sigma \varphi) \mathcal{G}^{(2,0)} + 4A^\mu A^\nu(\nabla_\mu \varphi)(\nabla^\rho \varphi)(\nabla_\nu \nabla_\rho \varphi + \nabla_\rho \nabla_\nu \varphi) \mathcal{G}^{(2,0)} \\ &\quad + 4A^\mu(\nabla_\mu \varphi)(\nabla_\nu \varphi)((\nabla_\rho \varphi)(\nabla^\rho A^\nu) + A^\nu A^\rho A^\sigma(\nabla_\sigma \nabla_\rho \varphi)) \mathcal{G}^{(2,0)} = 0, \end{aligned} \quad (\text{A3b})$$

$$\begin{aligned}
\frac{\delta S_{\text{EST}}}{\delta g^{\mu\nu}} \propto & 2R_{\mu\nu} + g_{\mu\nu} \left(-R + 2\kappa \left(\mathcal{G} - bA^\rho (\nabla_\rho A^\sigma) (\nabla_\sigma \varphi) + K_B \left(-(\nabla_\rho A_\sigma) + \nabla_\sigma A_\rho \right) (\nabla^\sigma A^\rho) \right) \right) \\
& + 2\kappa \left(-2A_\mu A_\nu \lambda + bA^\rho \left((\nabla_\nu \varphi) (\nabla_\rho A_\mu) + (\nabla_\mu \varphi) (\nabla_\rho A_\nu) \right) + bA_\nu (\nabla_\mu A^\rho) (\nabla_\rho \varphi) \right. \\
& + bA_\mu (\nabla_\nu A^\rho) (\nabla_\rho \varphi) - bA_\mu A_\nu (\nabla_\rho \nabla^\rho \varphi) - bA_\nu (\nabla_\rho \varphi) (\nabla^\rho A_\mu) - bA_\mu (\nabla_\rho \varphi) (\nabla^\rho A_\nu) \\
& + 2K_B \left(-(\nabla_\mu A^\rho) (\nabla_\nu A_\rho) + (\nabla_\nu A_\rho - \nabla_\rho A_\nu) (\nabla^\rho A_\mu) + (\nabla_\mu A_\rho) (\nabla^\rho A_\nu) \right) \\
& \left. - (A_\nu (\nabla_\mu \varphi) + A_\mu (\nabla_\nu \varphi)) \mathcal{G}^{(0,1)} - 2 \left((\nabla_\mu \varphi) (\nabla_\nu \varphi) + A^\rho (A_\nu (\nabla_\mu \varphi) + A_\mu (\nabla_\nu \varphi)) (\nabla_\rho \varphi) \right) \mathcal{G}^{(1,0)} \right) = 0. \quad (\text{A3c})
\end{aligned}$$

In Eqs. (A3a) to (A3c) we use the notation $\mathcal{G}^{(m,n)}$ to represent the m th partial derivative with respect to the first argument and the n th partial derivative with respect to the second argument of $\mathcal{G}(\mathcal{Y}, \mathcal{Q})$. By contracting Eq. (A3a) with an extra factor of A_μ and using Eq. (18), we obtain an algebraic equation for the Lagrange multiplier λ ,

$$\begin{aligned}
2\lambda = & -bJ^\nu (\nabla_\nu \varphi) + 2K_B A^\mu (\nabla_\nu \nabla_\mu A^\nu) + bA^\mu A^\nu (\nabla_\nu \nabla_\mu \varphi) - 2K_B A^\mu (\nabla_\nu \nabla^\nu A_\mu) \\
& - (A^\mu \nabla_\mu \varphi) \left[-b(\nabla_\nu A^\nu) - \mathcal{G}^{(0,1)} + 2A^\nu (\nabla_\nu \varphi) (K_B - 2 - \mathcal{G}^{(0,1)}) \right]. \quad (\text{A4})
\end{aligned}$$

B DETAILS OF COMPONENT EQUATIONS

Definitions. — In this appendix, we present all the non-trivial components of the field equations Eqs. (A3a) to (A3c), and at the same time we restrict the action Eq. (A1) to the specific form Eq. (11) for the function $\mathcal{F}(\mathcal{Y}, \mathcal{Q})$. The assumptions made about the behaviour of the fields are the minimal ones in Eqs. (19) and (20) required for spherical symmetry, along with the Ansatz Eq. (21) for the scalar. The arguments of the fields $\psi(r)$, $\chi(t)$, $\mathcal{M}(r)$, $\mathcal{N}(r)$, $\mathcal{R}(r)$, $\alpha(r)$ and $\mathcal{V}(\mathcal{Y})$ are suppressed, and a prime denotes differentiation with respect to each argument. We also define $S_k \equiv \sinh(k\alpha(r))$ and $C_k \equiv \cosh(k\alpha(r))$.

Equations. — There are seven equations in total:

$$\begin{aligned}
\frac{\delta S_{\text{EST}}^{\text{SZ}}}{\delta A_t} \propto & S_1 \left(4K_B \mathcal{R} C_1 S_1 \mathcal{M}' \mathcal{N}' - 8K_B C_1 S_1 \mathcal{N}' \mathcal{R}' + 4K_B \mathcal{R} S_1^2 \mathcal{M}' \alpha' - 4K_B \mathcal{R} S_1^2 \mathcal{N}' \alpha' - 8K_B S_1^2 \mathcal{R}' \alpha' - 4K_B \mathcal{R} C_1 S_1 \alpha'^2 \right. \\
& - 4e^{2\mathcal{M}-\mathcal{N}} \mathcal{R} S_1 \mathcal{F}_{20} Q_0^2 \chi' + 2e^{\mathcal{M}-\mathcal{N}} b \mathcal{R} C_2 Q_0 \mathcal{N}' \chi' - 4e^{\mathcal{M}-\mathcal{N}} b S_1^2 Q_0 \mathcal{R}' \chi' - 4e^{2\mathcal{M}-2\mathcal{N}} \mathcal{R} S_2 Q_0^2 \chi'^2 \\
& + 2e^{2\mathcal{M}-2\mathcal{N}} K_B \mathcal{R} S_2 Q_0^2 \chi'^2 + 2e^{2\mathcal{M}-2\mathcal{N}} \mathcal{R} S_2 \mathcal{F}_{20} Q_0^2 \chi'^2 + 4e^{\mathcal{M}-\mathcal{N}} K_B \mathcal{R} C_2 Q_0 \chi' \psi' - 4K_B \mathcal{R} S_1^2 \alpha'' \\
& - 4e^{\mathcal{M}} \mathcal{R} C_1 \mathcal{F}_{20} Q_0 \psi' + 2b \mathcal{R} C_1 S_1 \mathcal{M}' \psi' + 2b \mathcal{R} C_1 S_1 \mathcal{N}' \psi' - 4b C_1 S_1 \mathcal{R}' \psi' - 8e^{\mathcal{M}-\mathcal{N}} \mathcal{R} C_2 Q_0 \chi' \psi' \\
& + 4e^{\mathcal{M}-\mathcal{N}} \mathcal{R} C_2 \mathcal{F}_{20} Q_0 \chi' \psi' - 8 \mathcal{R} C_1 S_1 \psi'^2 + 4K_B \mathcal{R} C_1 S_1 \psi'^2 + 4 \mathcal{R} C_1 S_1 \mathcal{F}_{20} \psi'^2 - 4K_B \mathcal{R} C_1 S_1 \mathcal{N}'' \\
& - e^{2\mathcal{M}-2\mathcal{N}} b \mathcal{R} S_2 Q_0 \chi'' - 2b \mathcal{R} C_1 S_1 \psi'' - 2e^{2\mathcal{M}-2\mathcal{N}} \mathcal{R} S_2 Q_0^2 \chi'^2 \mathcal{V}' \\
& \left. - 4e^{\mathcal{M}-\mathcal{N}} \mathcal{R} C_2 Q_0 \chi' \psi' \mathcal{V}' - 4 \mathcal{R} C_1 S_1 \psi'^2 \mathcal{V}' \right) = 0, \quad (\text{B1a})
\end{aligned}$$

$$\begin{aligned}
\frac{\delta S_{\text{EST}}^{\text{SZ}}}{\delta A_r} \propto & C_1 \left(4K_B \mathcal{R} C_1 S_1 \mathcal{M}' \mathcal{N}' - 8K_B C_1 S_1 \mathcal{N}' \mathcal{R}' + 4K_B \mathcal{R} S_1^2 \mathcal{M}' \alpha' - 4K_B \mathcal{R} S_1^2 \mathcal{N}' \alpha' - 8K_B S_1^2 \mathcal{R}' \alpha' - 4K_B \mathcal{R} C_1 S_1 \alpha'^2 \right. \\
& - 4e^{2\mathcal{M}-\mathcal{N}} \mathcal{R} S_1 \mathcal{F}_{20} Q_0^2 \chi' + 2e^{\mathcal{M}-\mathcal{N}} b \mathcal{R} C_2 Q_0 \mathcal{N}' \chi' - 4e^{\mathcal{M}-\mathcal{N}} b S_1^2 Q_0 \mathcal{R}' \chi' - 4e^{2\mathcal{M}-2\mathcal{N}} \mathcal{R} S_2 Q_0^2 \chi'^2 \\
& + 2e^{2\mathcal{M}-2\mathcal{N}} K_B \mathcal{R} S_2 Q_0^2 \chi'^2 + 2e^{2\mathcal{M}-2\mathcal{N}} \mathcal{R} S_2 \mathcal{F}_{20} Q_0^2 \chi'^2 + 4e^{\mathcal{M}-\mathcal{N}} K_B \mathcal{R} C_2 Q_0 \chi' \psi' - 4K_B \mathcal{R} S_1^2 \alpha'' \\
& - 4e^{\mathcal{M}} \mathcal{R} C_1 \mathcal{F}_{20} Q_0 \psi' + 2b \mathcal{R} C_1 S_1 \mathcal{M}' \psi' + 2b \mathcal{R} C_1 S_1 \mathcal{N}' \psi' - 4b C_1 S_1 \mathcal{R}' \psi' - 8e^{\mathcal{M}-\mathcal{N}} \mathcal{R} C_2 Q_0 \chi' \psi' \\
& + 4e^{\mathcal{M}-\mathcal{N}} \mathcal{R} C_2 \mathcal{F}_{20} Q_0 \chi' \psi' - 8 \mathcal{R} C_1 S_1 \psi'^2 + 4K_B \mathcal{R} C_1 S_1 \psi'^2 + 4 \mathcal{R} C_1 S_1 \mathcal{F}_{20} \psi'^2 - 4K_B \mathcal{R} C_1 S_1 \mathcal{N}'' \\
& - e^{2\mathcal{M}-2\mathcal{N}} b \mathcal{R} S_2 Q_0 \chi'' - 2b \mathcal{R} C_1 S_1 \psi'' - 2e^{2\mathcal{M}-2\mathcal{N}} \mathcal{R} S_2 Q_0^2 \chi'^2 \mathcal{V}' \\
& \left. - 4e^{\mathcal{M}-\mathcal{N}} \mathcal{R} C_2 Q_0 \chi' \psi' \mathcal{V}' - 4 \mathcal{R} C_1 S_1 \psi'^2 \mathcal{V}' \right) = 0, \quad (\text{B1b})
\end{aligned}$$

$$\begin{aligned}
\frac{\delta S_{\text{EST}}^{\text{SZ}}}{\delta \varphi} \propto & 4e^{3\mathcal{M}} \mathcal{R} S_1 \mathcal{F}_{20} Q_0 \mathcal{N}' + 2e^{2\mathcal{M}} b \mathcal{R} C_1^2 \mathcal{M}' \mathcal{N}' - 2e^{2\mathcal{M}} b \mathcal{R} C_1^2 \mathcal{N}'^2 + 8e^{3\mathcal{M}} S_1 \mathcal{F}_{20} Q_0 \mathcal{R}' - 4e^{2\mathcal{M}} b C_1^2 \mathcal{N}' \mathcal{R}' + 4e^{3\mathcal{M}} \mathcal{R} C_1 \mathcal{F}_{20} Q_0 \alpha' \\
& + 2e^{2\mathcal{M}} b \mathcal{R} C_1 S_1 \mathcal{M}' \alpha' - 3e^{2\mathcal{M}} b \mathcal{R} S_2 \mathcal{N}' \alpha' - 2e^{2\mathcal{M}} b S_2 \mathcal{R}' \alpha' - 2e^{2\mathcal{M}} b \mathcal{R} C_2 \alpha'^2 - 4e^{3\mathcal{M}-\mathcal{N}} S_2 \mathcal{F}_{20} Q_0 \mathcal{R}' \chi' + 8e^{2\mathcal{M}} C_1^2 \mathcal{R}' \psi' \mathcal{V}' \\
& - 4e^{3\mathcal{M}-\mathcal{N}} \mathcal{R} C_2 \mathcal{F}_{20} Q_0 \alpha' \chi' + 4e^{2\mathcal{M}} \mathcal{R} S_1^2 \mathcal{F}_{20} \mathcal{M}' \psi' - 4e^{2\mathcal{M}} \mathcal{R} S_1^2 \mathcal{F}_{20} \mathcal{N}' \psi' - 8e^{2\mathcal{M}} S_1^2 \mathcal{F}_{20} \mathcal{R}' \psi' - 4e^{2\mathcal{M}} \mathcal{R} S_2 \mathcal{F}_{20} \alpha' \psi'
\end{aligned}$$

$$\begin{aligned}
& -e^{2\mathcal{M}}b\mathcal{R}\mathcal{N}'' - e^{2\mathcal{M}}b\mathcal{R}\mathcal{C}_2\mathcal{N}'' - e^{2\mathcal{M}}b\mathcal{R}\mathcal{S}_2\alpha'' - 4e^{4\mathcal{M}-2\mathcal{N}}\mathcal{R}\mathcal{C}_1^2\mathcal{F}_{20}\mathcal{Q}_0\chi'' - 4e^{2\mathcal{M}}\mathcal{R}\mathcal{S}_1^2\mathcal{F}_{20}\psi'' + 4e^{2\mathcal{M}}\mathcal{R}\mathcal{S}_2\alpha'\psi'\mathcal{V}' \\
& + 4e^{3\mathcal{M}-\mathcal{N}}\mathcal{S}_2\mathcal{Q}_0\mathcal{R}'\lambda'\mathcal{V}' + 4e^{3\mathcal{M}-\mathcal{N}}\mathcal{R}\mathcal{C}_2\mathcal{Q}_0\alpha'\lambda'\mathcal{V}' - 4e^{2\mathcal{M}}\mathcal{R}\mathcal{C}_1^2\mathcal{M}'\psi'\mathcal{V}' + 4e^{2\mathcal{M}}\mathcal{R}\mathcal{C}_1^2\mathcal{N}'\psi'\mathcal{V}' + 4e^{2\mathcal{M}}\mathcal{R}\mathcal{C}_1^2\psi''\mathcal{V}' \\
& + 4e^{4\mathcal{M}-2\mathcal{N}}\mathcal{R}\mathcal{S}_1^2\mathcal{Q}_0\chi''\mathcal{V}' - 8e^{3\mathcal{M}-3\mathcal{N}}\mathcal{R}\mathcal{C}_1\mathcal{S}_1^3\mathcal{Q}_0\mathcal{N}'\chi'^3\mathcal{V}'' + 8e^{3\mathcal{M}-3\mathcal{N}}\mathcal{R}\mathcal{C}_1^2\mathcal{S}_1^2\mathcal{Q}_0\alpha'\chi'^3\mathcal{V}'' - 2e^{2\mathcal{M}-2\mathcal{N}}\mathcal{R}\mathcal{S}_2^2\mathcal{Q}_0\mathcal{M}'\chi'^2\psi'\mathcal{V}'' \\
& - 4e^{2\mathcal{M}-2\mathcal{N}}\mathcal{R}\mathcal{S}_2^2\mathcal{Q}_0\mathcal{N}'\chi'^2\psi'\mathcal{V}'' + 2e^{2\mathcal{M}-2\mathcal{N}}\mathcal{R}\mathcal{S}_2\mathcal{Q}_0^2\alpha'\chi'^2\psi'\mathcal{V}'' + 6e^{2\mathcal{M}-2\mathcal{N}}\mathcal{R}\mathcal{C}_2\mathcal{S}_2\mathcal{Q}_0\alpha'\chi'^2\psi'\mathcal{V}'' - 8\mathcal{R}\mathcal{C}_1^4\mathcal{M}'\psi'^3\mathcal{V}'' \\
& - 8e^{\mathcal{M}-\mathcal{N}}\mathcal{R}\mathcal{C}_1^2\mathcal{S}_2\mathcal{Q}_0\mathcal{M}'\chi'\psi'^2\mathcal{V}'' - 4e^{\mathcal{M}-\mathcal{N}}\mathcal{R}\mathcal{C}_1^2\mathcal{S}_2\mathcal{Q}_0\mathcal{N}'\chi'\psi'^2\mathcal{V}'' - 4e^{\mathcal{M}-\mathcal{N}}\mathcal{R}\mathcal{C}_1^2\mathcal{Q}_0\alpha'\chi'\psi'^2\mathcal{V}'' + 8\mathcal{R}\mathcal{C}_1^3\mathcal{S}_1\alpha'\psi'^3\mathcal{V}'' \\
& + 12e^{\mathcal{M}-\mathcal{N}}\mathcal{R}\mathcal{C}_1^2\mathcal{C}_2\mathcal{Q}_0\alpha'\chi'\psi'^2\mathcal{V}'' + 2e^{2\mathcal{M}-2\mathcal{N}}\mathcal{R}\mathcal{S}_2^2\mathcal{Q}_0\chi'^2\psi''\mathcal{V}'' + 8e^{\mathcal{M}-\mathcal{N}}\mathcal{R}\mathcal{C}_1^2\mathcal{S}_2\mathcal{Q}_0\chi'\psi'\psi''\mathcal{V}'' + 8\mathcal{R}\mathcal{C}_1^4\psi^2\psi''\mathcal{V}'' \\
& + 8e^{4\mathcal{M}-4\mathcal{N}}\mathcal{R}\mathcal{S}_1^4\mathcal{Q}_0\chi'^2\chi''\mathcal{V}'' + 16e^{3\mathcal{M}-3\mathcal{N}}\mathcal{R}\mathcal{C}_1\mathcal{S}_1^3\mathcal{Q}_0\chi'\psi'\chi''\mathcal{V}'' + 2e^{2\mathcal{M}-2\mathcal{N}}\mathcal{R}\mathcal{S}_2^2\mathcal{Q}_0\psi'^2\chi''\mathcal{V}'' = 0, \tag{B1c}
\end{aligned}$$

$$\begin{aligned}
\frac{\delta S_{\text{EST}}^{\text{SZ}}}{\delta g^{tt}} \propto & 4e^{2\mathcal{M}} + 4e^{2\mathcal{M}}\mathcal{R}^2\kappa\mathcal{F}_{20}\mathcal{Q}_0^2 - 4e^{2\mathcal{M}}\mathcal{R}\kappa^2\mathcal{V} + 8K_B\mathcal{R}^2\kappa\mathcal{C}_1^4\mathcal{M}'\mathcal{N}' - 4K_B\mathcal{R}^2\kappa\mathcal{C}_1^2\mathcal{N}'^2 + 8\mathcal{R}\mathcal{M}'\mathcal{R}' - 4\mathcal{R}'^2 - 8\mathcal{R}\mathcal{R}'' \\
& - 16K_B\mathcal{R}\mathcal{C}_1^4\mathcal{N}'\mathcal{R}' + 8K_B\mathcal{R}^2\kappa\mathcal{C}_1^3\mathcal{S}_1\mathcal{M}'\alpha' - 8K_B\mathcal{R}^2\kappa\mathcal{C}_1^3\mathcal{S}_1\mathcal{N}'\alpha' - 4K_B\mathcal{R}^2\kappa\mathcal{S}_2\mathcal{N}'\alpha' - 16K_B\mathcal{R}\kappa\mathcal{C}_1^3\mathcal{S}_1\mathcal{R}'\alpha' \\
& - 8K_B\mathcal{R}^2\kappa\mathcal{C}_1^4\alpha'^2 - 4K_B\mathcal{R}^2\kappa\mathcal{S}_1^2\alpha'^2 + 8e^{2\mathcal{M}-\mathcal{N}}\mathcal{R}^2\kappa\mathcal{C}_1\mathcal{F}_{20}\mathcal{Q}_0^2\chi' - 8e^{2\mathcal{M}-\mathcal{N}}\mathcal{R}^2\kappa\mathcal{C}_1^3\mathcal{F}_{20}\mathcal{Q}_0^2\chi' - 8b\mathcal{R}\kappa\mathcal{C}_1^4\mathcal{R}'\psi' \\
& + 8e^{\mathcal{M}-\mathcal{N}}b\mathcal{R}^2\kappa\mathcal{C}_1^3\mathcal{S}_1\mathcal{Q}_0\mathcal{N}'\chi' - 2e^{\mathcal{M}-\mathcal{N}}b\mathcal{R}^2\kappa\mathcal{S}_2\mathcal{Q}_0\mathcal{N}'\chi' - 4e^{\mathcal{M}-\mathcal{N}}b\mathcal{R}^2\kappa\mathcal{S}_1^2\mathcal{Q}_0\alpha'\chi' + 2b\mathcal{R}^2\kappa\mathcal{C}_1^2\mathcal{C}_2\mathcal{N}'\psi' \\
& - 8e^{\mathcal{M}-\mathcal{N}}b\mathcal{R}\kappa\mathcal{C}_1^3\mathcal{S}_1\mathcal{Q}_0\mathcal{R}'\chi' - 4e^{\mathcal{M}-\mathcal{N}}b\mathcal{R}^2\kappa\mathcal{C}_1^2\mathcal{Q}_0\alpha'\chi' + 4b\mathcal{R}^2\kappa\mathcal{C}_1^4\mathcal{M}'\psi' - 2b\mathcal{R}^2\kappa\mathcal{C}_1^2\mathcal{N}'\psi' - 2b\mathcal{R}^2\kappa\mathcal{S}_2\alpha'\psi' \\
& - 16e^{2\mathcal{M}-2\mathcal{N}}\mathcal{R}^2\kappa\mathcal{C}_1^4\mathcal{Q}_0^2\chi'^2 + 8e^{2\mathcal{M}-2\mathcal{N}}K_B\mathcal{R}^2\kappa\mathcal{C}_1^4\mathcal{Q}_0^2\chi'^2 - 12e^{2\mathcal{M}-2\mathcal{N}}\mathcal{R}^2\kappa\mathcal{C}_1^2\mathcal{F}_{20}\mathcal{Q}_0^2\chi'^2 - 8e^{\mathcal{M}}\mathcal{R}^2\kappa\mathcal{S}_1\mathcal{F}_{20}\mathcal{Q}_0\psi' \\
& + 8e^{2\mathcal{M}-2\mathcal{N}}\mathcal{R}^2\kappa\mathcal{C}_1^4\mathcal{F}_{20}\mathcal{Q}_0^2\chi'^2 - 8e^{\mathcal{M}}\mathcal{R}^2\kappa\mathcal{C}_1^2\mathcal{S}_1\mathcal{F}_{20}\mathcal{Q}_0\psi' - 32e^{\mathcal{M}-\mathcal{N}}\mathcal{R}^2\kappa\mathcal{C}_1^3\mathcal{S}_1\mathcal{Q}_0\chi'\psi' - 4e^{\mathcal{M}-\mathcal{N}}\mathcal{R}^2\kappa\mathcal{S}_2\mathcal{F}_{20}\mathcal{Q}_0\chi'\psi' \\
& + 16e^{\mathcal{M}-\mathcal{N}}\mathcal{R}^2\kappa\mathcal{C}_1^3\mathcal{S}_1\mathcal{F}_{20}\mathcal{Q}_0\chi'\psi' + 16e^{\mathcal{M}-\mathcal{N}}K_B\mathcal{R}^2\kappa\mathcal{C}_1^3\mathcal{S}_1\mathcal{Q}_0\chi'\psi' - 4\mathcal{R}^2\kappa\mathcal{S}_2^2\psi'^2 + 2K_B\mathcal{R}^2\kappa\mathcal{S}_2^2\psi'^2 + 2\mathcal{R}^2\kappa\mathcal{S}_2^2\mathcal{F}_{20}\psi'^2 \\
& + 4\mathcal{R}^2\kappa\mathcal{S}_1^2\mathcal{F}_{20}\psi'^2 - 8K_B\mathcal{R}^2\kappa\mathcal{C}_1^4\mathcal{N}'' - 8K_B\mathcal{R}^2\kappa\mathcal{C}_1^3\mathcal{S}_1\alpha'' - 16e^{\mathcal{M}-\mathcal{N}}\mathcal{R}^2\kappa\mathcal{C}_1^3\mathcal{S}_1\mathcal{Q}_0\chi'\psi'\mathcal{V}' + 8e^{\mathcal{M}-\mathcal{N}}\mathcal{R}^2\kappa\mathcal{S}_2\mathcal{Q}_0\chi'\psi'\mathcal{V}' \\
& + 4e^{2\mathcal{M}-2\mathcal{N}}b\mathcal{R}^2\kappa\mathcal{C}_1^2\mathcal{Q}_0\lambda'' - 4e^{2\mathcal{M}-2\mathcal{N}}\mathcal{R}^2\kappa\mathcal{C}_1^4\mathcal{Q}_0\chi'' - 4b\mathcal{R}^2\kappa\mathcal{C}_1^2\psi'' - b\mathcal{R}^2\kappa\mathcal{S}_2^2\psi'' - 8e^{2\mathcal{M}-2\mathcal{N}}\mathcal{R}^2\kappa\mathcal{C}_1^4\mathcal{Q}_0\lambda'^2\mathcal{V}' \\
& - 8e^{2\mathcal{M}-2\mathcal{N}}\mathcal{R}^2\kappa\mathcal{Q}_0\chi'^2\mathcal{V}' + 16e^{2\mathcal{M}-2\mathcal{N}}\mathcal{R}^2\kappa\mathcal{C}_1^2\mathcal{Q}_0\lambda'^2\mathcal{V}' - 8\mathcal{R}^2\kappa\mathcal{C}_1^2\mathcal{S}_1^2\psi'^2\mathcal{V}' = 0, \tag{B1d}
\end{aligned}$$

$$\begin{aligned}
\frac{\delta S_{\text{EST}}^{\text{SZ}}}{\delta g^{tr}} \propto & -16K_B\mathcal{R}\mathcal{C}_1^3\mathcal{S}_1\mathcal{M}'\mathcal{N}' + 32K_B\mathcal{C}_1^3\mathcal{S}_1\mathcal{N}'\mathcal{R}' - 16K_B\mathcal{R}\mathcal{C}_1^2\mathcal{S}_1^2\mathcal{M}'\alpha' + 16K_B\mathcal{R}\mathcal{C}_1^2\mathcal{S}_1^2\mathcal{N}'\alpha' + 32K_B\mathcal{C}_1^2\mathcal{S}_1^2\mathcal{R}'\alpha' \\
& + 4K_B\mathcal{R}\mathcal{S}_2\alpha'^2 + 2K_B\mathcal{R}\mathcal{S}_4\alpha'^2 - 12e^{2\mathcal{M}-\mathcal{N}}\mathcal{R}\mathcal{S}_1\mathcal{F}_{20}\mathcal{Q}_0^2\chi' + 4e^{\mathcal{M}-\mathcal{N}}b\mathcal{R}\mathcal{S}_2\mathcal{Q}_0\alpha'\chi' + 8e^{2\mathcal{M}-2\mathcal{N}}\mathcal{R}\mathcal{S}_2\mathcal{Q}_0^2\chi'^2 \\
& + 4e^{2\mathcal{M}-\mathcal{N}}\mathcal{R}\mathcal{S}_3\mathcal{F}_{20}\mathcal{Q}_0^2\chi' - 16e^{\mathcal{M}-\mathcal{N}}b\mathcal{R}\mathcal{C}_1^2\mathcal{S}_1^2\mathcal{Q}_0\mathcal{N}'\chi' + 16e^{\mathcal{M}-\mathcal{N}}b\mathcal{C}_1^2\mathcal{S}_1^2\mathcal{Q}_0\mathcal{R}'\chi' - 4e^{2\mathcal{M}-2\mathcal{N}}K_B\mathcal{R}\mathcal{S}_2\mathcal{Q}_0^2\chi'^2 \\
& + 4e^{2\mathcal{M}-2\mathcal{N}}\mathcal{R}\mathcal{S}_4\mathcal{Q}_0^2\chi'^2 - 2e^{2\mathcal{M}-2\mathcal{N}}K_B\mathcal{R}\mathcal{S}_4\mathcal{Q}_0^2\chi'^2 + 4e^{2\mathcal{M}-2\mathcal{N}}\mathcal{R}\mathcal{S}_2\mathcal{F}_{20}\mathcal{Q}_0^2\chi'^2 - 2e^{2\mathcal{M}-2\mathcal{N}}\mathcal{R}\mathcal{S}_4\mathcal{F}_{20}\mathcal{Q}_0^2\chi'^2 \\
& + 12e^{\mathcal{M}}\mathcal{R}\mathcal{C}_1\mathcal{F}_{20}\mathcal{Q}_0\psi' + 4e^{\mathcal{M}}\mathcal{R}\mathcal{C}_3\mathcal{F}_{20}\mathcal{Q}_0\psi' - 8b\mathcal{R}\mathcal{C}_1^3\mathcal{S}_1\mathcal{N}'\psi' + 16b\mathcal{C}_1^3\mathcal{S}_1\mathcal{R}'\psi' - 8e^{\mathcal{M}-\mathcal{N}}\mathcal{R}\mathcal{Q}_0\chi'\psi' \\
& - 8b\mathcal{R}\mathcal{C}_1^3\mathcal{S}_1\mathcal{M}'\psi' - 2K_B\mathcal{R}\mathcal{S}_4\psi'^2 - 4\mathcal{R}\mathcal{S}_2\mathcal{F}_{20}\psi'^2 - 2\mathcal{R}\mathcal{S}_4\mathcal{F}_{20}\psi'^2 + 4K_B\mathcal{R}\mathcal{S}_2\mathcal{N}'' + 2K_B\mathcal{R}\mathcal{S}_4\mathcal{N}'' \\
& + 4e^{\mathcal{M}-\mathcal{N}}K_B\mathcal{R}\mathcal{Q}_0\chi'\psi' + 8e^{\mathcal{M}-\mathcal{N}}\mathcal{R}\mathcal{C}_4\mathcal{Q}_0\chi'\psi' - 4e^{\mathcal{M}-\mathcal{N}}K_B\mathcal{R}\mathcal{C}_4\mathcal{Q}_0\chi'\psi' - 12e^{\mathcal{M}-\mathcal{N}}\mathcal{R}\mathcal{F}_{20}\mathcal{Q}_0\chi'\psi' \\
& - 4e^{\mathcal{M}-\mathcal{N}}\mathcal{R}\mathcal{C}_4\mathcal{F}_{20}\mathcal{Q}_0\chi'\psi' - 8\mathcal{R}\mathcal{S}_2\psi^2 + 4K_B\mathcal{R}\mathcal{S}_2\psi'^2 + 2e^{2\mathcal{M}-2\mathcal{N}}\mathcal{R}\mathcal{S}_4\mathcal{Q}_0^2\chi'^2\mathcal{V}' + e^{2\mathcal{M}-2\mathcal{N}}b\mathcal{R}\mathcal{S}_4\mathcal{Q}_0\chi'' \\
& - 4e^{\mathcal{M}-\mathcal{N}}\mathcal{R}\mathcal{Q}_0\chi'\psi'\mathcal{V}' + 4e^{\mathcal{M}-\mathcal{N}}\mathcal{R}\mathcal{C}_4\mathcal{Q}_0\chi'\psi'\mathcal{V}' + 4\mathcal{R}\mathcal{S}_2\psi'^2\mathcal{V}' + 2\mathcal{R}\mathcal{S}_4\psi'^2\mathcal{V}' - 4e^{2\mathcal{M}-2\mathcal{N}}\mathcal{R}\mathcal{S}_2\mathcal{Q}_0^2\chi'^2\mathcal{V}' \\
& - 2K_B\mathcal{R}\alpha'' + 2K_B\mathcal{R}\mathcal{C}_4\alpha'' - 2e^{2\mathcal{M}-2\mathcal{N}}b\mathcal{R}\mathcal{S}_2\mathcal{Q}_0\chi'' + 2b\mathcal{R}\mathcal{S}_2\psi'' + b\mathcal{R}\mathcal{S}_4\psi'' + 4\mathcal{R}\mathcal{S}_4\psi'^2 = 0, \tag{B1e}
\end{aligned}$$

$$\begin{aligned}
\frac{\delta S_{\text{EST}}^{\text{SZ}}}{\delta g^{rr}} \propto & -4e^{2\mathcal{M}} - 4e^{2\mathcal{M}}\mathcal{R}^2\kappa\mathcal{F}_{20}\mathcal{Q}_0^2 + 4e^{2\mathcal{M}}\mathcal{R}^2\kappa\mathcal{V} + 8K_B\mathcal{R}^2\kappa\mathcal{C}_1^2\mathcal{S}_1^2\mathcal{M}'\mathcal{N}' + 4K_B\mathcal{R}^2\kappa\mathcal{C}_1^2\mathcal{N}'^2 - 4K_B\mathcal{R}\kappa\mathcal{S}_2^2\mathcal{N}'\mathcal{R}' \\
& + 8\mathcal{R}\mathcal{N}'\mathcal{R}' + 4\mathcal{R}'^2 + 8K_B\mathcal{R}^2\kappa\mathcal{C}_1\mathcal{S}_1^3\mathcal{M}'\alpha' + 6K_B\mathcal{R}^2\kappa\mathcal{S}_2\mathcal{N}'\alpha' + 4K_B\mathcal{R}^2\kappa\mathcal{S}_1^2\alpha'^2 - 16K_B\mathcal{R}\kappa\mathcal{C}_1\mathcal{S}_1^3\mathcal{R}'\alpha' \\
& - K_B\mathcal{R}^2\kappa\mathcal{S}_4\mathcal{N}'\alpha' - 2K_B\mathcal{R}^2\kappa\mathcal{S}_2^2\alpha'^2 + 8e^{2\mathcal{M}-\mathcal{N}}\mathcal{R}^2\kappa\mathcal{C}_1\mathcal{F}_{20}\mathcal{Q}_0^2\chi' - 8e^{2\mathcal{M}-\mathcal{N}}\mathcal{R}^2\kappa\mathcal{C}_1\mathcal{S}_1^2\mathcal{F}_{20}\mathcal{Q}_0^2\chi' \\
& + e^{\mathcal{M}-\mathcal{N}}b\mathcal{R}^2\kappa\mathcal{S}_4\mathcal{Q}_0\mathcal{N}'\chi' - 8e^{\mathcal{M}-\mathcal{N}}b\mathcal{R}\kappa\mathcal{C}_1\mathcal{S}_1^3\mathcal{Q}_0\mathcal{R}'\chi' - 4e^{2\mathcal{M}-2\mathcal{N}}\mathcal{R}^2\kappa\mathcal{S}_2^2\mathcal{Q}_0^2\chi'^2 - 8e^{\mathcal{M}}\mathcal{R}^2\kappa\mathcal{S}_1\mathcal{F}_{20}\mathcal{Q}_0\psi' \\
& + 2e^{2\mathcal{M}-2\mathcal{N}}\mathcal{R}^2\kappa\mathcal{S}_2^2\mathcal{Q}_0^2\chi'^2 + 4b\mathcal{R}^2\kappa\mathcal{C}_1^2\mathcal{S}_1^2\mathcal{M}'\psi' + 4b\mathcal{R}^2\kappa\mathcal{C}_1^4\mathcal{N}'\psi' - 8b\mathcal{R}\kappa\mathcal{C}_1^2\mathcal{S}_1^2\mathcal{R}'\psi' + 2b\mathcal{R}^2\kappa\mathcal{S}_2\alpha'\psi'
\end{aligned}$$

$$\begin{aligned}
& -4e^{2\mathcal{M}-2\mathcal{N}}\mathcal{R}^2\kappa C_1^2\mathcal{F}_{20}Q_0^2\chi'^2 + 2e^{2\mathcal{M}-2\mathcal{N}}\mathcal{R}^2\kappa S_2^2\mathcal{F}_{20}Q_0^2\chi'^2 + 4e^{\mathcal{M}-\mathcal{N}}\mathcal{R}^2\kappa S_2\mathcal{F}_{20}Q_0\chi'\psi' - 16\mathcal{R}^2\kappa S_1^4\psi'^2 \\
& -8e^{\mathcal{M}}\mathcal{R}^2\kappa S_1^3\mathcal{F}_{20}Q_0\psi' + 8K_B\mathcal{R}^2\kappa S_1^4\psi'^2 + 12\mathcal{R}^2\kappa S_1^2\mathcal{F}_{20}\psi'^2 + 8\mathcal{R}^2\kappa S_1^4\mathcal{F}_{20}\psi'^2 - 2K_B\mathcal{R}^2\kappa S_2^2\mathcal{N}'' \\
& -32e^{\mathcal{M}-\mathcal{N}}\mathcal{R}^2\kappa C_1S_1^3Q_0\chi'\psi' + 16e^{\mathcal{M}-\mathcal{N}}K_B\mathcal{R}^2\kappa C_1S_1^3Q_0\chi'\psi' + 16e^{\mathcal{M}-\mathcal{N}}\mathcal{R}^2\kappa C_1S_1^3\mathcal{F}_{20}Q_0\chi'\psi' \\
& -8\mathcal{R}^2\kappa C_1S_1^3\alpha'' + 4e^{2\mathcal{M}-2\mathcal{N}}b\mathcal{R}^2\kappa S_1^2Q_0\chi'' - e^{2\mathcal{M}-\mathcal{N}}b\mathcal{R}^2\kappa S_2^2Q_0\chi'' - 4b\mathcal{R}^2\kappa S_1^2\psi'' - 4b\mathcal{R}^2\kappa S_1^4\psi'' \\
& -8e^{2\mathcal{M}-2\mathcal{N}}\mathcal{R}^2\kappa C_1^2S_1^2Q_0^2\chi'^2\mathcal{V}' - 16e^{\mathcal{M}-\mathcal{N}}\mathcal{R}^2\kappa C_1S_1^3Q_0\chi'\psi'\mathcal{V}' - 16\mathcal{R}^2\kappa S_1^2\psi'^2\mathcal{V}' - 8\mathcal{R}^2\kappa S_1^4\psi'^2\mathcal{V}' \\
& -8e^{\mathcal{M}-\mathcal{N}}\mathcal{R}^2\kappa S_2Q_0\chi'\psi'\mathcal{V}' - 8\mathcal{R}^2\kappa\psi'^2\mathcal{V}' = 0,
\end{aligned} \tag{B1f}$$

$$\begin{aligned}
\frac{\delta S_{\text{ÆST}}^{\text{SZ}}}{\delta g^{\theta\theta}} & \propto e^{2\mathcal{M}}\mathcal{R}\kappa\mathcal{F}_{20}Q_0^2 - e^{2\mathcal{M}}\mathcal{R}\kappa\mathcal{V} + K_B\mathcal{R}\kappa C_1^2\mathcal{N}'^2 + K_B\mathcal{R}\kappa S_2\mathcal{N}'\alpha' + K_B\mathcal{R}\kappa S_1^2\alpha'^2 - \mathcal{R}\mathcal{N}'^2 + \mathcal{M}'\mathcal{R}' - \mathcal{N}'\mathcal{R}' \\
& -2e^{2\mathcal{M}-\mathcal{N}}\mathcal{R}\kappa C_1\mathcal{F}_{20}Q_0^2\chi' + e^{\mathcal{M}-\mathcal{N}}b\mathcal{R}\kappa C_1S_1Q_0\mathcal{N}'\chi' + e^{\mathcal{M}-\mathcal{N}}b\mathcal{R}\kappa S_1^2Q_0\alpha'\chi' + e^{2\mathcal{M}-2\mathcal{N}}\mathcal{R}\kappa C_1^2\mathcal{F}_{20}Q_0^2\chi'^2 \\
& -2e^{\mathcal{M}}\mathcal{R}\kappa S_1\mathcal{F}_{20}Q_0\psi' + b\mathcal{R}\kappa C_1^2\mathcal{N}'\psi' + b\mathcal{R}\kappa C_1S_1\alpha'\psi' + e^{\mathcal{M}-\mathcal{N}}\mathcal{R}\kappa S_2\mathcal{F}_{20}Q_0\chi'\psi' + \mathcal{R}\kappa S_1^2\mathcal{F}_{20}\psi'^2 - \mathcal{R}\mathcal{N}'' \\
& + \mathcal{R}\mathcal{M}'\mathcal{N}' - \mathcal{R}'' = 0.
\end{aligned} \tag{B1g}$$

Note that these equations are not all independent. Specifically, Eq. (B1a) and Eq. (B1b) are related by the normalization condition Eq. (18), whilst Eqs. (B1d) to (B1g) are related by the Bianchi identity.

C CONSERVATION OF ÆTHER ACCELERATION

Einstein-æther case. — In this appendix we prove the result in Eq. (37), that in EÆ theory the æther acceleration is generically a conserved current if *both* the æther and the spacetime geometry are static. The first step in this proof is to prepare certain results. From Eq. (18) it follows that $\nabla_\mu(A^\nu A_\nu) = 0$. This implies $A^\nu \nabla_\mu A_\nu = 0$, and hence

$$F_{\mu\nu}A^\nu \equiv \nabla_\mu(A_\nu A^\nu) - A^\nu \nabla_\nu A_\mu = -J_\mu. \tag{C1}$$

Next, we start to use the two staticity conditions. Staticity of the spacetime implies the existence of a global timelike Killing vector ξ^μ . Staticity of the æther and the condition in Eq. (18) implies that A^μ describes precisely the field of four-velocities of static observers. Accordingly, we may write

$$A^\mu = \frac{\xi^\mu}{N}, \quad N \equiv \sqrt{-\xi^\alpha \xi_\alpha}, \tag{C2}$$

where N is the lapse function. Together with the identification in Eq. (C2), Killing's identity $\nabla_\alpha \nabla^\alpha \xi^\mu \equiv -R^\mu_\nu \xi^\nu$ implies that the divergence of the æther acceleration defined in Eq. (23) is related to the Ricci tensor by

$$\nabla_\mu J^\mu = -R_{\mu\nu}A^\mu A^\nu. \tag{C3}$$

So far, the only field equation that has been exploited is Eq. (18). Thus, assuming only that the model in question can be thought of as GR coupled (minimally) to some matter in such a way that doubly static solutions exist, then one can express Eq. (C3) in terms of the matter stress-energy tensor $T_{\mu\nu}$ by using the Einstein equations $R_{\mu\nu} - \frac{1}{2}Rg_{\mu\nu} = \kappa T_{\mu\nu}$, so that

$$\nabla_\mu J^\mu = -\kappa \left(T_{\mu\nu}A^\mu A^\nu + \frac{1}{2}T \right), \tag{C4}$$

where $T \equiv T^\mu_\mu$ is the trace of the stress-energy tensor. In practice, of course, both Eqs. (7) and (9) satisfy these assumptions about the model, and so the Komar-type construction in Eq. (C4) is valid for both EÆ and ÆST theories. Lastly, static æther is hypersurface orthogonal in static spacetime. This means that, in the kinematical decomposition of the congruence of A^μ , the expansion, shear and twist all vanish, which allows us to write $\nabla_\mu A_\nu = -A_\mu J_\nu$ and $F_{\mu\nu} = -A_\mu J_\nu + A_\nu J_\mu$. This leads to a further result (as quoted already in Eq. (23))

$$F_{\mu\nu}F^{\mu\nu} = -2J_\mu J^\mu, \tag{C5}$$

which can also be used in obtaining Eq. (30). We now apply Eqs. (C1), (C4) and (C5) to the specific case of EÆ theory. We will work in terms of the æther coupling K_B as introduced in Eq. (7), but of course the results also apply to the 'effective' coupling K_B^{eff} defined in Eq. (35). From Eq. (7) we deduce

$$\kappa T_{\mu\nu} = K_B F_{\mu\alpha}F_\nu{}^\alpha - \frac{K_B}{4}g_{\mu\nu}F_{\alpha\beta}F^{\alpha\beta} + \lambda A_\mu A_\nu, \tag{C6}$$

and by using Eqs. (18) and (C1) the relevant scalars formed from Eq. (C6) are found to be

$$\kappa T_{\mu\nu} A^\mu A^\nu = K_B J_\mu J^\mu + \frac{K_B}{4} F_{\mu\nu} F^{\mu\nu} + \lambda, \quad \kappa T = -\lambda. \quad (\text{C7})$$

When Eq. (C7) is substituted into Eq. (C4), we conclude

$$\nabla_\mu J^\mu = -K_B J_\mu J^\mu - \frac{K_B}{4} F_{\mu\nu} F^{\mu\nu} - \frac{1}{2}\lambda. \quad (\text{C8})$$

As mentioned in Section II C, the æther field equation itself generally allows the Lagrange multiplier λ to be determined on the shell. In the case of the EÆ theory in Eq. (7), an application of Eq. (C1) then reduces this result to

$$\lambda = K_B \nabla_\mu J^\mu + \frac{K_B}{2} F_{\mu\nu} F^{\mu\nu}. \quad (\text{C9})$$

After substituting Eq. (C9) into Eq. (C8) and making one last application of Eq. (C5), we find

$$(2 + K_B) \nabla_\mu J^\mu = 0, \quad (\text{C10})$$

and Eq. (C10) implies Eq. (37).

Æther-scalar-tensor case. — For the ÆST action in Eq. (17), it is possible to replace the scalar-tensor kinetic interaction $-F^{\mu\nu} A_\nu$ with J_μ . The energy momentum tensor is then easier to compute, and Eq. (C6) is replaced by Eq. (A2)

$$\begin{aligned} \kappa T_{\mu\nu} = & K_B F_{\mu\alpha} F_\nu{}^\alpha - \frac{K_B}{4} g_{\mu\nu} F^{\alpha\beta} F_{\alpha\beta} + \frac{b}{2} (F^\beta{}_\nu A_\mu \nabla_\beta \psi + F^\beta{}_\mu A_\nu \nabla_\beta \psi - J_\mu \nabla_\nu \psi - J_\nu \nabla_\mu \psi) + \frac{b}{2} g_{\mu\nu} J^\alpha \nabla_\alpha \psi \\ & + \nabla_\mu \psi \nabla_\nu \psi \frac{d\mathcal{V}}{d\mathcal{Y}} - \frac{1}{2} g_{\mu\nu} \mathcal{V}(\mathcal{Y}) + \lambda A_\mu A_\nu. \end{aligned} \quad (\text{C11})$$

By using Eqs. (18) and (C1), and $A^\mu J_\mu = A^\mu \nabla_\mu \psi = 0$, the relevant scalars in Eq. (C7) are replaced by

$$\kappa T_{\mu\nu} A^\mu A^\nu = \frac{K_B}{2} J_\mu J^\mu + \frac{b}{2} J^\mu \nabla_\mu \psi + \frac{1}{2} \mathcal{V}(\mathcal{Y}) + \lambda, \quad \kappa T = \mathcal{V} \frac{d\mathcal{V}}{d\mathcal{Y}} - 2\mathcal{V}(\mathcal{Y}) - \lambda. \quad (\text{C12})$$

When Eq. (C12) is substituted into Eq. (C4), we conclude

$$\nabla_\mu J^\mu = -\frac{K_B}{2} J_\mu J^\mu - \frac{b}{2} J^\mu \nabla_\mu \psi + \frac{1}{2} \mathcal{V}(\mathcal{Y}) - \frac{1}{2} \mathcal{V} \frac{d\mathcal{V}}{d\mathcal{Y}} - \frac{1}{2} \lambda. \quad (\text{C13})$$

From Eq. (A4), and using the fact that $A^\mu \nabla_\mu \psi = 0$, we have

$$\lambda = -b J^\mu \nabla_\mu \psi + K_B \nabla_\mu J^\mu - K_B J^\mu J_\mu. \quad (\text{C14})$$

Finally, by combining Eqs. (C13) and (C14) we obtain the analogue of Eq. (C10)

$$(2 + K_B) \nabla_\mu J^\mu = \mathcal{V}(\mathcal{Y}) - \mathcal{V} \frac{d\mathcal{V}}{d\mathcal{Y}}. \quad (\text{C15})$$

Therefore, Eq. (C15) shows that $\nabla_\mu J^\mu = 0$, if $\mathcal{V}(\mathcal{Y}) \propto \mathcal{Y}$, consistent with the assumptions that lead to Eq. (26).

D DETAILS OF EXACT SOLUTIONS

New definitions. — In this appendix, we shall use the following definitions for convenience:

$$\Upsilon \equiv \frac{d\mathcal{N}}{dr}, \quad \mathcal{P} \equiv \frac{d\psi}{dr}. \quad (\text{D1})$$

Ellis–Bronnikov drainhole. — Without loss of generality, we refine Eq. (19) to a genuinely Schwarzschild-like coordinate system so that

$$\mathcal{R} = r. \quad (\text{D2})$$

After substituting Eqs. (22), (26), (28) and (D2), the only field equations that do not vanish are Eqs. (B1c), (B1d), (B1f) and (B1g). These are respectively given by

$$-b\Upsilon + ar \frac{d\mathcal{P}}{dr} + a\mathcal{P} \left(2 + r\Upsilon - r \frac{d\mathcal{M}}{dr} \right) - \frac{b}{2}r \left(\Upsilon^2 + \frac{d\Upsilon}{dr} - \Upsilon \frac{d\mathcal{M}}{dr} \right) = 0, \quad (\text{D3a})$$

$$-1 + e^{2\mathcal{M}} - \frac{r}{2} \left(2b\mathcal{P} + ar\mathcal{P}^2 + br \frac{d\mathcal{P}}{dr} + K_B \left(\Upsilon(4 + r\Upsilon) + 2r \frac{d\Upsilon}{dr} \right) \right) + r \frac{d\mathcal{M}}{dr} \left(2 + \frac{b}{2}r\mathcal{P} + K_B r\Upsilon \right) = 0, \quad (\text{D3b})$$

$$1 - e^{2\mathcal{M}} + r \left(2\Upsilon + \frac{r}{2} (-a\mathcal{P}^2 + b\mathcal{P}\Upsilon + K_B \Upsilon^2) \right) = 0, \quad (\text{D3c})$$

$$\Upsilon - \frac{d\mathcal{M}}{dr} + r \left(\frac{a}{2}\mathcal{P}^2 - \frac{b}{2}\mathcal{P}\Upsilon + \frac{d\Upsilon}{dr} - \Upsilon \left(-1 + \frac{K_B}{2} \right) \Upsilon + \frac{d\mathcal{M}}{dr} \right) = 0. \quad (\text{D3d})$$

In Eqs. (D3a) to (D3d) we have used Eq. (D1). One can combine Eqs. (D3b) and (D3c) to eliminate $e^{2\mathcal{M}}$. The remaining equations can be rearranged to yield

$$\frac{d\mathcal{M}}{dr} = \frac{a}{2}r\mathcal{P}^2 - \frac{b}{2}r\mathcal{P}\Upsilon - \Upsilon \left(1 + \frac{K_B}{2}r\Upsilon \right), \quad (\text{D4a})$$

$$\frac{d\Upsilon}{dr} = \Upsilon \left(\frac{d\mathcal{M}}{dr} - \Upsilon - \frac{2}{r} \right), \quad (\text{D4b})$$

$$\frac{d\mathcal{P}}{dr} = \mathcal{P} \left(\frac{d\mathcal{M}}{dr} - \Upsilon - \frac{2}{r} \right). \quad (\text{D4c})$$

From Eqs. (D4b) and (D4c), it is obvious that $\mathcal{P} = q\Upsilon$ for some constant q , and this leads to our conjecture in Eqs. (34) and (36). With reference to Eq. (35), the system in Eqs. (D3c) and (D4b) becomes

$$r \frac{d\Upsilon}{dr} = -2\Upsilon - 2r\Upsilon^2 - \frac{K_B^{\text{eff}}}{2}r^2\Upsilon^3, \quad e^{2\mathcal{M}} = 1 + 2r\Upsilon + \frac{K_B^{\text{eff}}}{2}r^2\Upsilon^2. \quad (\text{D5})$$

Notice that the final equations of motion in Eq. (D5) are precisely the same as those of EÆ theory in Schwarzschild-like coordinates, see, for example, [66, 78]. This is the result which was to be proven, but we now go beyond it so as to actually solve Eq. (D5). The choice of Schwarzschild-like coordinate in Eq. (D2) is generally different from the radial gauge Eq. (24) chosen to present the results in Sections III and IV. We will now define a new radial coordinate σ , a special case of the general r we have been using hitherto, which we require to be proportional to the affine parameter of radial null geodesics. More concretely, this choice of radial coordinate is motivated as follows. In general, we want our gauge condition in Eq. (24) to always apply in the coordinates we happen to be using, and so it needs to be revised accordingly whenever we rescale the radial coordinate. Starting, therefore, from the general r coordinate, we want to move to the new radial coordinate σ in which this gauge condition is actually $g_{tt} = -1/g_{\sigma\sigma}$. In terms of the original r coordinate, this implies $-\mathcal{N} = \mathcal{M} + \ln(dr/d\sigma)$ which, taking derivatives with respect to σ , becomes a differential equation for $r(\sigma)$

$$\frac{d^2r}{d\sigma^2} = -\frac{dr}{d\sigma} \left(\frac{d\mathcal{N}}{d\sigma} + \frac{d\mathcal{M}}{d\sigma} \right). \quad (\text{D6})$$

This is precisely the radial geodesic equation following from Eq. (19), which motivates this choice of radial coordinate. Accordingly, we move from r to σ as defined in Eq. (D6). We then further have the identities

$$\frac{d\mathcal{N}}{d\sigma} \equiv \frac{d\mathcal{N}}{dr} \frac{dr}{d\sigma}, \quad \frac{d^2\mathcal{N}}{d\sigma^2} \equiv -\left(\frac{d\mathcal{N}}{d\sigma} \right)^2 - \frac{d\mathcal{N}}{d\sigma} \frac{d\mathcal{M}}{d\sigma} + \frac{d^2\mathcal{N}}{dr^2} \left(\frac{dr}{d\sigma} \right)^2. \quad (\text{D7})$$

By combining Eqs. (D5) to (D7), we find that Eqs. (D4a) and (D4b) become

$$\frac{d^2\mathcal{N}}{d\sigma^2} = -\frac{2}{r} \frac{dr}{d\sigma} \frac{d\mathcal{N}}{d\sigma} - 2 \left(\frac{d\mathcal{N}}{d\sigma} \right)^2, \quad \frac{d^2r}{d\sigma^2} = \frac{K_B^{\text{eff}}}{2}r \left(\frac{d\mathcal{N}}{d\sigma} \right)^2. \quad (\text{D8})$$

The solution to the first equation of Eq. (D8) is

$$r^2 = c_1^2 e^{-2\mathcal{N}} \frac{d\sigma}{d\mathcal{N}}, \quad (\text{D9})$$

for some integration constant c_1 . Once again, Eq. (D9) is independent of the coupling parameters in the action and is a result of the conservation of the æther acceleration in Eq. (37). Now from Eqs. (D8) and (D9), we find

$$\frac{d\mathcal{N}}{d\sigma} = \frac{2c_3}{2(\sigma + c_2)^2 + (K_B^{\text{eff}} - 2)c_3^2}, \quad (\text{D10})$$

with further integration constants c_2 and c_3 . For the case of the Ellis–Bronnikov drainhole, one can choose $c_2 = 0$ and assume Eq. (42). By re-labelling σ as r and integrating Eq. (D10) with the constraints of Minkowski geometry at spatial infinity, we then recover the line-element function in Eq. (43a). The other function Eq. (43b) is obtained from Eqs. (D2) and (D9), again with appropriate integration constants.

First extended Eling–Jacobson solution. — The Eling–Jacobson wormhole is obtained as the special case of Eq. (D10) where $c_2 = -c_3\sqrt{1 - K_B^{\text{eff}}/2}$, and Eq. (39) is also assumed instead of Eq. (42).

Anti-Ellis–Bronnikov solution. — Whilst the Eling–Jacobson solution was a special case of the solution branch which led also to the Ellis–Bronnikov drainhole, we now start afresh by considering quite a different branch, in which Eq. (D1) holds true. The condition in Eq. (48) translates to

$$\Upsilon = 0. \quad (\text{D11})$$

With Eqs. (24) and (D11), one is forced to have constant $\mathcal{M} = -\mathcal{N}$, which we satisfy by the simple choice $\mathcal{M} = \mathcal{N} = 0$, which is already consistent with the first equality in Eq. (49). To proceed, Eq. (B1c) now reduces to

$$-\frac{2}{\mathcal{R}} \frac{d\mathcal{R}}{dr} = \frac{1}{\mathcal{P}} \frac{d\mathcal{P}}{dr}. \quad (\text{D12})$$

Now Eq. (D12) implies that

$$\mathcal{P} = c_1 \mathcal{R}^{-2}, \quad (\text{D13})$$

for some constant c_1 . After substituting Eq. (D13), it can be seen that Eqs. (B1d), (B1f) and (B1g) all reduce to the same differential equation

$$\left(\frac{d\mathcal{R}}{dr}\right)^2 = 1 + \frac{ac_1^2}{2\mathcal{R}^2}. \quad (\text{D14})$$

A solution to Eq. (D14) is

$$\mathcal{R}^2 = -\frac{ac_1^2}{2} + r^2. \quad (\text{D15})$$

Therefore, with the identification $\ell^2 = ac_1^2/2$ in Eq. (D15) the second equality in Eq. (49) is also recovered.

Second extended Eling–Jacobson solution. — By substituting Eqs. (22), (26) and (52) into Eq. (B1b) we obtain

$$e^{\mathcal{M}+\mathcal{N}} \mathcal{R} \frac{d\chi}{dt} \left(b \frac{d\mathcal{N}}{dr} - 2a \frac{d\psi}{dr} \right) = 0. \quad (\text{D16})$$

For regions where the coordinates in Eq. (19) are non-singular, Eq. (D16) evidently gives rise to Eq. (29). As a consequence, if χ is non-constant we must have

$$\frac{d\psi}{dr} = \frac{b}{2a} \frac{d\mathcal{N}}{dr}. \quad (\text{D17})$$

We then substitute Eq. (D17) into Eqs. (B1d), (B1f) and (B1g), and combine these equations to yield

$$2 \frac{d\mathcal{R}}{dr} \frac{d\mathcal{M}}{dr} + \mathcal{R} \left[\frac{d^2\mathcal{M}}{dr^2} - 2 \left(\frac{d\mathcal{M}}{dr} \right)^2 \right] = 0. \quad (\text{D18})$$

Notice that Eqs. (D8) and (D18) have a similar form, except that \mathcal{N} is replaced with $-\mathcal{M}$ in Eq. (D8), as expected from Eq. (24). Hence, the implication is that

$$\mathcal{R} = c_1 e^{\mathcal{M}} \sqrt{-\frac{dr}{d\mathcal{M}}}, \quad (\text{D19})$$

for some integration constant c_1 . Notice that Eq. (D19) is independent of the coupling constant K_B and a . In fact, Eq. (D19) is a result of the conservation of the æther current in Eq. (37). By substituting Eq. (D19) into Eq. (B1f) we obtain

$$\frac{d\mathcal{M}}{dr} = -\frac{c_1^2}{r^2} \left(1 - \frac{2c_3}{r}\right)^{-1}, \quad c_3 \equiv c_1^2 \sqrt{\frac{(2 - K_B)\lambda_s}{2(1 + \lambda_s)}}. \quad (\text{D20})$$

The solution to Eq. (D20), in combination with Eq. (24), leads to the geometry in Eqs. (56a) and (56b). One can substitute Eqs. (56a), (56b) and (57) back to verify that all the other field equations are satisfied.

Cosmological solution. — When Eqs. (22), (24) and (53) are imposed, and Eq. (28) is relaxed, we find that Eq. (B1e) is satisfied by the first equality in Eq. (58). Meanwhile, Eq. (B1b) reduces to

$$\mathcal{Q}_0 \mathcal{R} \frac{d\mathcal{V}}{d\mathcal{Y}} \frac{d\psi}{dr} = 0. \quad (\text{D21})$$

From Eq. (D21), we are obliged to set Eq. (59) which, when substituted into Eqs. (B1f) and (B1g), respectively gives

$$-1 + \Lambda \kappa \mathcal{R}^2 + \left(\frac{d\mathcal{R}}{dr}\right)^2 = 0, \quad \Lambda \kappa \mathcal{R} + \frac{d^2 \mathcal{R}}{dr^2} = 0. \quad (\text{D22})$$

The equations in Eq. (D22) are satisfied by the second equality in Eq. (58) which, when substituted into Eq. (B1d), gives rise to

$$2\sqrt{\kappa\Lambda} \cos(\sqrt{\kappa\Lambda}r) (K_B - 2) \frac{d\psi}{dr} + \sin(\sqrt{\kappa\Lambda}r) \left[2\kappa\Lambda + (K_B - 2) \frac{d^2\psi}{dr^2}\right] = 0. \quad (\text{D23})$$

It can then be shown that Eq. (60) solves Eq. (D23).

E MORE LIKE BLACK HOLES THAN WORMHOLES

Null singularity. — In this appendix, we discuss the nature and extendibility of the solution in Eqs. (45a) and (45b) beyond the hypersurface that appears to be a Killing horizon. We first assume the condition in Eq. (24), which allows r to be interpreted as the affine parameter of the radial null geodesics. Now let

$$k^\mu \equiv \frac{dx^\mu}{dr}, \quad [x^\mu] \equiv [t, r, \theta, \phi], \quad (\text{E1})$$

be the tangent vector to such geodesics for coordinates x^μ in Eq. (19). Then from Eqs. (19) and (24), the particular curvature scalar considered in [66] takes the form

$$R_{\mu\nu} k^\mu k^\nu = -\frac{2}{\mathcal{R}} \frac{d^2 \mathcal{R}}{dr^2}. \quad (\text{E2})$$

If, as $r \rightarrow r_S$, the volume element behaves as $\mathcal{R} \approx r e^{\mathcal{H}} \left(1 - \frac{r_S}{r}\right)^\epsilon$, where $\mathcal{H} \equiv \mathcal{H}(r)$ is regular at $r = r_S$ and $\epsilon < 0$, then the curvature scalar in Eq. (E2) takes the form

$$R_{\mu\nu} k^\mu k^\nu \approx -\frac{2r_S^2 \epsilon(\epsilon - 1)}{r^2 (r - r_S)^2} + \frac{4[r + r_S(\epsilon - 1)]}{r(r - r_S)} \frac{d\mathcal{H}}{dr} - 2 \left(\frac{d\mathcal{H}}{dr}\right)^2 - 2 \frac{d^2 \mathcal{H}}{dr^2}. \quad (\text{E3})$$

According to Eq. (E3), this scalar quantity always diverges at this hypersurface, i.e. it is a null singularity.

No conformal rescaling. — We will now show this singular behavior can be removed by some conformal transformations. However, for the solutions discussed in this paper, the cost of doing so is either shifting this surface to a null-infinity, or making the Ricci scalar diverges. Suppose, for some regular $\mathcal{K} \equiv \mathcal{K}(r)$, the conformal factor we are looking for takes the form $\Omega \equiv \Omega(r)$ so that

$$g_{\mu\nu} \mapsto \Omega^2 g_{\mu\nu}, \quad \Omega \equiv e^{\mathcal{K}} \left(1 - \frac{r_S}{r}\right)^\gamma. \quad (\text{E4})$$

The condition from Eq. (E4) that the hypersurface is not shifted to null-infinity is $2\gamma > -1$. Next, the cases in which the singularity in Eq. (E3) can be removed are

$$(\mathcal{K}(r) = \Delta(r) - \ln(r)) \wedge \gamma \in \{\epsilon - 1, -\epsilon\}. \quad (\text{E5})$$

The function $\Delta(r)$ introduced in Eq. (E5) is the solution to the following differential equation,

$$0 = 2 \left(r - r_S \cdot \frac{\epsilon(\epsilon - 1)}{\gamma} \right) \cdot \Delta' + 2(r + r_S \cdot (\epsilon - 1)) \cdot \mathcal{H}' - r(r - r_S) \cdot (\Delta'^2 - \mathcal{H}'^2) + r(r - r_S) \cdot (\Delta'' + \mathcal{H}''). \quad (\text{E6})$$

From Eq. (E6), one immediately has $\Delta = -\mathcal{H}$ for the case $\gamma = -\epsilon$. The case when $\gamma = \epsilon - 1$ is more complicated, but one can always find the series expansion of Δ in the vicinity of the horizon in terms of \mathcal{H} and its derivatives. Under such choices of γ and \mathcal{K} , the scalar defined by Eq. (E2) is guaranteed to be 0 at $r = r_S$, hence the singularity is removed. Notice that the choice $\gamma = \epsilon - 1$ clearly violates the condition $2\gamma > 1$ since $\epsilon < 0$ by assumption. Which means, if one choose $\gamma = \epsilon - 1$, the cost of removing this singularity is shifting the surface at $r = r_S$ to a null-infinity. We now turn our attention to the Ricci scalar for the choice $\gamma = -\epsilon$.

General curvature scalars. — We now study the behavior of other scalar quantities near this surface, noting how Eqs. (19) and (24) imply for some regular, nonzero $\mathcal{T} \equiv \mathcal{T}(r)$

$$e^{2\mathcal{N}} \approx \mathcal{T} \left(1 - \frac{r_S}{r} \right)^\beta, \quad \mathcal{R} \approx r e^{\mathcal{H}} \left(1 - \frac{r_S}{r} \right)^\epsilon. \quad (\text{E7})$$

From Eq. (E7) we conclude that, after the conformal transformation described by Eq. (E4), the scalar concomitants of the curvature tensor and the metric behave as (including the tidal stress experienced by radial massive observer)

$$\mathcal{S}(R^\mu{}_{\nu\sigma\lambda}, g_{\mu\nu}) \propto \left(1 - \frac{r_S}{r} \right)^{\mu\zeta}, \quad \mu > 0, \quad \zeta \equiv \min(-2\epsilon - 2\gamma, \beta - 2\gamma - 2). \quad (\text{E8})$$

For example, Eq. (E8) implies if one choose $\gamma = -\epsilon$, the Ricci scalar

$$R \propto \left(1 - \frac{r_S}{r} \right)^\zeta, \quad \zeta \equiv \min(0, \beta + 2\epsilon - 2) = \beta + 2\epsilon - 2. \quad (\text{E9})$$

For the case under consideration, we have $\beta > 0$ and $\epsilon < 0$. Thus, for the choice $\gamma = -\epsilon$, $\zeta < 0$ if and only if $\beta + 2\epsilon > 2$. In such cases, the curvature scalar and Eq. (E2) are all regularized, and the null hypersurface is not a null-infinity.

For the solution discussed in Eq. (2), one always has $\beta + 2\epsilon = -2 < 2$. Hence, the cost of removing the singular behavior in the scalar Eq. (E2) for $\gamma = -\epsilon$ for this solution is to make the Ricci scalar singular, which makes the hypersurface defined by $r = r_S$ remain a null singularity. We thus showed that, for spacetime described by Eq. (2), near the null hypersurface $r = r_S$, the following three conditions **cannot** be simultaneously satisfied via a conformal transformation of spacetime:

- the surface can be reached by radial photon within finite amount of its affine parameter;
- the scalar defined in Eq. (E2) is regular;
- the curvature scalar is regular.

We therefore can safely conclude that the radial photon geodesics are non-extendible at the null hypersurface $r = r_S$.

For the physical spacetime, from Eq. (E8) with $\gamma = 0$, the null surface at $r = r_S$ is not a curvature singularity, if and only if

$$\beta > 2. \quad (\text{E10})$$

In the solution of Eq. (45a), the condition in Eq. (E10) is

$$\beta = \frac{2}{\sqrt{4 - 2K_B^{\text{eff}}}} > 2, \quad (\text{E11})$$

and Eq. (E11) gives $3/2 < K_B^{\text{eff}} < 2$. Within this range, the curvature scalar is regular at $r = r_S$.